CHAPTER VII

BEAM TRANSPORT AND MANIPULATION (OR PURIFICATION)

7.1 Introduction

The layout of the beam transport lines has been deeply changed from the 2009 up to now

The first simulation of the beam transport from the ion source to the Beam Cooler, started in November 2009 using the program TRACEWIN.

In February 2010 a new configuration from the ion source to the platform of the RFQ beam cooler was carried out using the program code GIOS [1], which simulates the Wien Filter placed on the production platform and also take account of nonlinear effects up to the 3rd order. At that time we studied also the optic of the HRMS and the optic of the beam transport line from the HRMS to PIAVE injector.

Finally in the 2011 the transport line was heavily redesigned to take account of the decision to reduce the High Voltage of the production target from the previous 260 kV down to 40 kV.

Here we present a short description of the two early version of the beam transport line explaining the reasons of the evolution then in the following sessions we focus to describe the optic of present beam line design.

The layout of the line designed in 2010 is shown in Fig. 7.1. The two productions targets are placed on two H.V. platforms to deliver beams with energy of 260 keV. At that time was already decided to install a Wien Filter on each platform to stop the majority of the radioactive contaminants that come out from the target ion source (TIS) complex right in the production area that is well shielded.

Despite this decision the transverse focusing effects of the WIEN Filter on the beam were not simulated because TRACEWIN was not able to simulate this device. Anyway the effects of the WIEN Filter in our case are expected to be small.

Moreover, it was verified that with the help of the Wien Filter and using the first triplet of electrostatic quadrupoles, placed immediately after the TIS, is possible to achieve a good focusing of the beam in the orizonthal plane. This configuration allow to achieve a mass selection with a resolution* better than $\Delta M/M = 0.01$. Here and in the follow the meaning of mass resolution or mass resolving power are quite different of the usual meanings. The usual definition for mass resolving power is the ability of a optical analysing system to identify two different mass. For this reason the mass resolving power of an optical system at first order is defined as $R_{16}/X_0\ R_{11}$, where R_{16} is the dispersion of the system X_0 is the full width at half maximum (FWHM) of the beam at the object position and R_{11} is the magnification of the system. In our case we want use a separator or a beam selector. In particular we want minimize the contaminants in the beam that we have selected. For this reason what we like is to have a complete separation of two different mass. At first order our mass resolving power is 2 times smaller at first order, because we like to use for the mass resolving power of mass separator system the following definition $R_{16}/(2X_0\ R_{11})$. In the case were higher order are considered we assume as width of the beam at the selection plane the Full Width at one tenth of Maximum (FWtM).

The use of the WIEN filter allows to maintain almost all the radioactive elements produced in the TIS inside the platform area. Thereby the risk of contamination of all the devices installed along the beam transport line (pipe line, vacuum chamber of quadrupoles and dipoles, vacuum pumps, diagnostics etc…) outside the production area is greatly reduced.

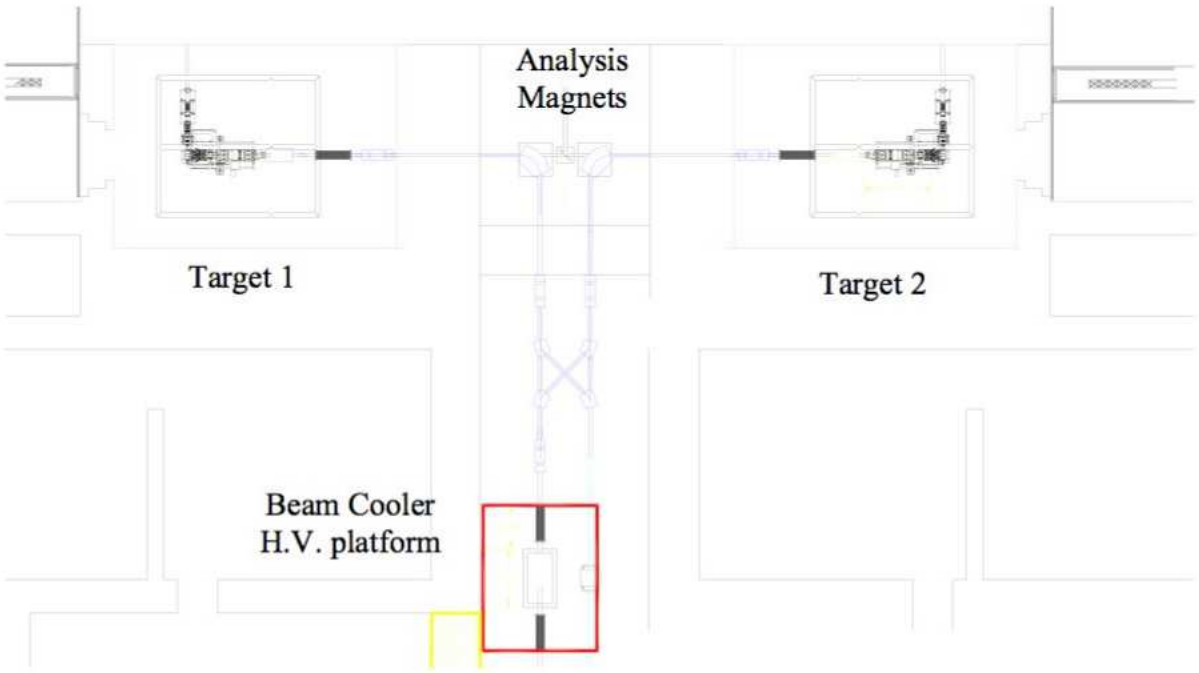

Figure 7.1: *Previous layout of the beam transport lines from production platforms to the beam cooler platform, year 2009.*

The layout shown in Figure 1, consists of the two productions area that contain the TIS, the focusing triplet the Wien Filter and the accelerating column, then in the room between the two productions area there are two analysis magnets with bending angle of 90°, one for each production platform.

At that time, we plan to use each one of the two lines to delivery low-energy radioactive beams to two different experimental rooms, one at low energy and with low mass resolving power another at higher energy and with high mass resolving power.

The High Resolution Mass Separator (HRMS) proposed for the SPES project at 2009 was just the HRMS of EXCYT project with just bending radius of the main dipoles a 10% bigger.

More accurate functional analysis of the various components of the SPES project highlighted additional problems that suggest us to change this previous layout.

The main problems of this configuration were:

Here a list:

- Small room between the concrete wall of the production area and the entrance face of the dipoles at 90°. This small distance does not allow the insertion of a cryogenic trap in front of each dipole. These traps are used to lock the neutral radioactive elements coming out from the TIS in gaseous form, which could flow out along the transport lines.The increased size of the platform-Beam RFQ Cooler, which interferes heavily with the presence of the two independent lines.
- Although the mass resolving power of the Wien filter system + dipole analysis may be even greater than 300 this value, in many cases, it is not enough to guarantee the purity of the isotope beams to be used in the room measuring at low energy. The end users of this beams like to have a purified beam coming out by the High Resolving Mass Separator with mass resolving power >20.000.
- Looking forward at the facility operations, we like to use the two platforms in alternate mode in order to allow the dismantling of the used production sources, after a period of "radioactivity cool down" of 12-15 days. Conversely, the possibility of working with both

platforms simultaneously has little chance of being achieved, given the need to wait 12-15 days before to change the TIS.

- Last but not the least the area and cost of the facility are reduced.

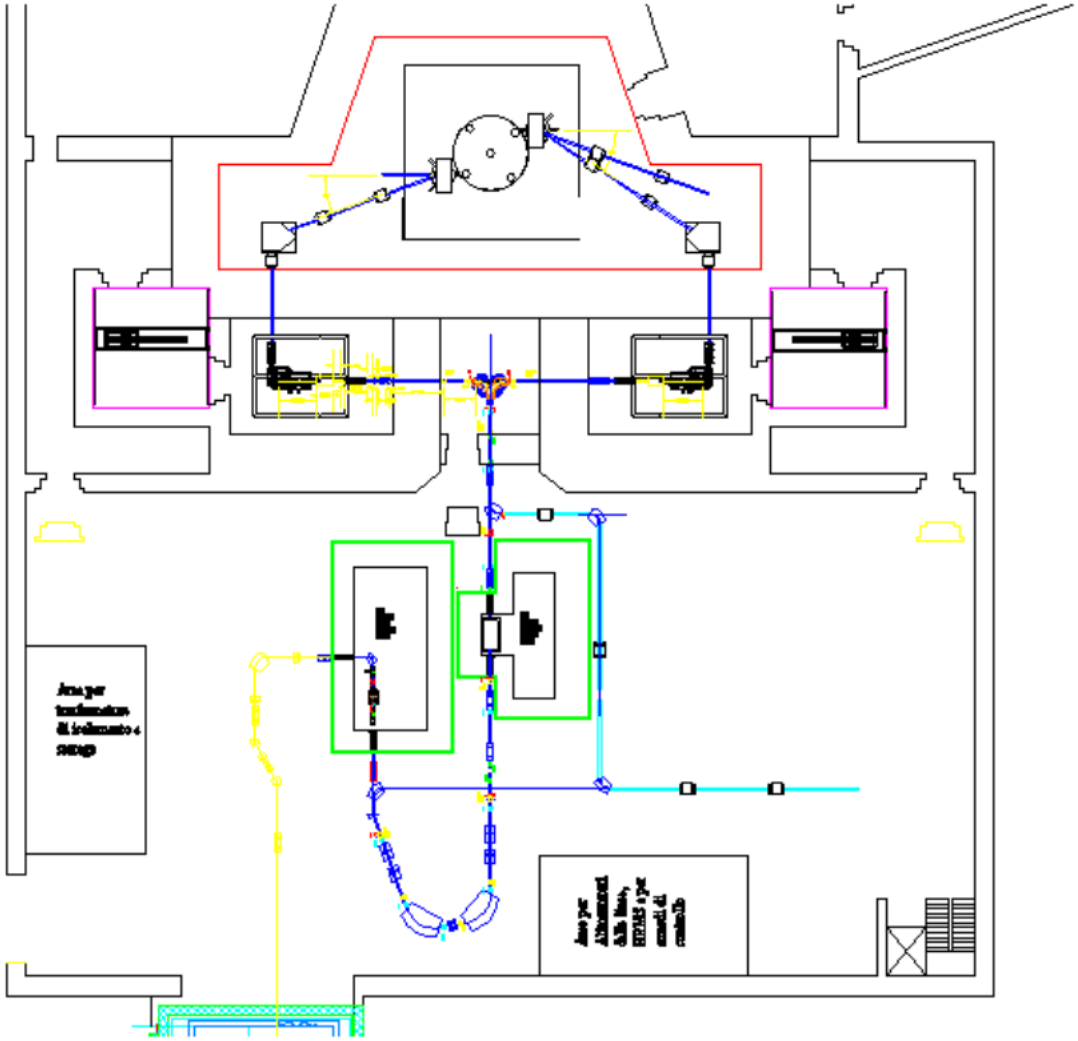

Figure 7.2: *Second layout of the beam transport lines from production platforms to the RFQ beam cooler platform, year 2010.*

Therefore, the layout of the beam transport lines from the production rooms at the Cooler beam has been modified and simplified according to fig. 7.2. The main change was to replace the two independent 90° bending magnet with a single magnet with two beam lines entrance, one at -90° and another at 90° respect to the exit line, see fig. 7.3. This solution allows increase the radius of curvature of the dipole from the previous value of 600 mm at the value of 800 mm to achieve an higher mass resolving power. Moreover, the distance between the shielding walls of the production platforms and the entrance of the analysis magnet is increased of a further 1 m, so there is enough room to install two cryogenic traps along the beam line arriving from the two productions area and before the 90° bending magnet. A third cryogenic trap, just for redundancy, may also be installed along the exit beam line of the 90° dipole. Of course the beam optic of this beam line was also studied, but is not here described for sake of simplicity.

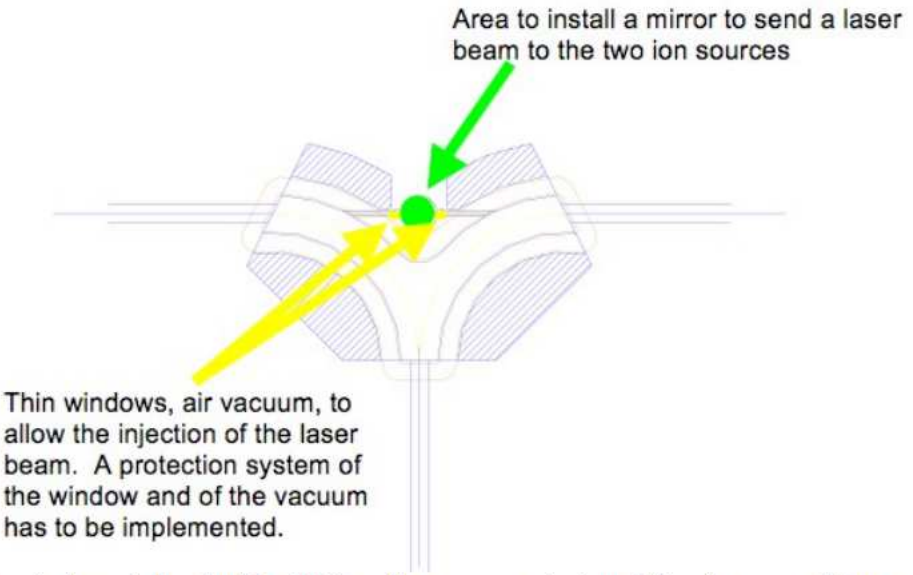

Figure 7.3: *Particular of the double 90° bending magnet designed for the second layout. The magnet design take account of the request to use a laser beam to drive the ion source with the Light Ionization Selective (LIS), year 2010.*

The long beam line transport complex from the ion source to PIAVE pre-accelerator is shown in fig. 7.4. In this figure is possible to see the position of the main components of the beam transport and purification system: The Beam Cooler, the HRMS and the Charge Breeder, necessary to deliver ion beam with the proper M/q ratio to allow the acceleration by the following LINAC. The transport of high charge ions along the long beam transport line requires to design a pumping system able to achieve a vacuum of about 10^{-6} Pa. The length of the beam line is about 130 m. The optic of this line was also studied, but for sake of simplicity is not described here.

From fig. 7.4 it is evident that the purification and preparation system proposed needs two additional H.V. platforms, one for the Beam Cooler and another for the Charge Breeder.

Along the 2011 the project was deeply modified for three main reasons:

- The use of high voltage platform, higher than 200 kV, inside an environment with high level of radioactivity and in particular the high ionization effect produced by the high power incident beam on the target was demonstrate to be not safe, so it was decided to reduce the platform voltage at lower values between 40-60 kV;
- use a new RFQ as preinjector to achieve independent injector for radioactive beam and stable beam. Moreover this solution avoid to use PIAVE RFQ that pose serious problem of the long transport line or alternatively for the needs to move PIAVE from the present position to a new area in the so called “Terza Sala”;
- reduce the size of the building to save money;
- Install the charge breeder and the new RFQ near the main linac ALPI, inside the existing “Terza Sala”, about 50 m away from the HRMS.

The result of this heavy redesign is shown in fig. 7.5 and 7.6. The main changes are: the reduction of the acceleration voltage of the radioactive ion beams, the Beam Cooler and the HRMS will be installed rotated of 90° respect to the previous configuration. The charge breeder was moved inside the so called “Terza Sala”. The beam cooler and the Charge Breeder don’t need to have H.V. platforms. To maintain the high mass resolving power of 40.000 the HRMS it is convenient that the beam energy will be as high as possible, for this reason the HRMS will be installed on a 220 kV H.V. platform.

Figure 7.4: *Layout of the beam transport line from the Beam cooler to the injection in PIAVE RFQ. The positions of Beam Cooler, HRMS, Charge Breeder and beam transfer line are shown (2010).*

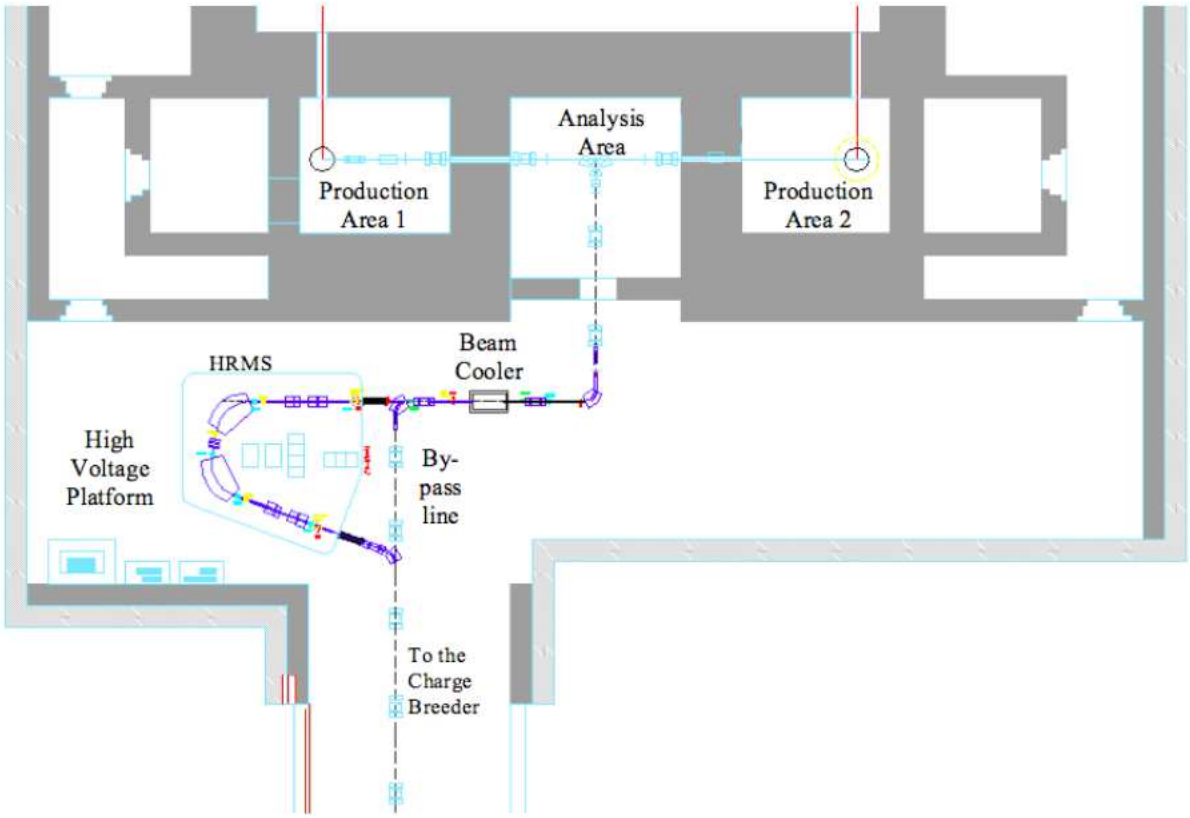

Figure 7.5: *Updated layout of the beam transport line, from the ion source to the beam line to inject the beam into the charge breeder. The Analysis dipoles, Beam Cooler, By-pass line and HRMS positions are shown (2012).*

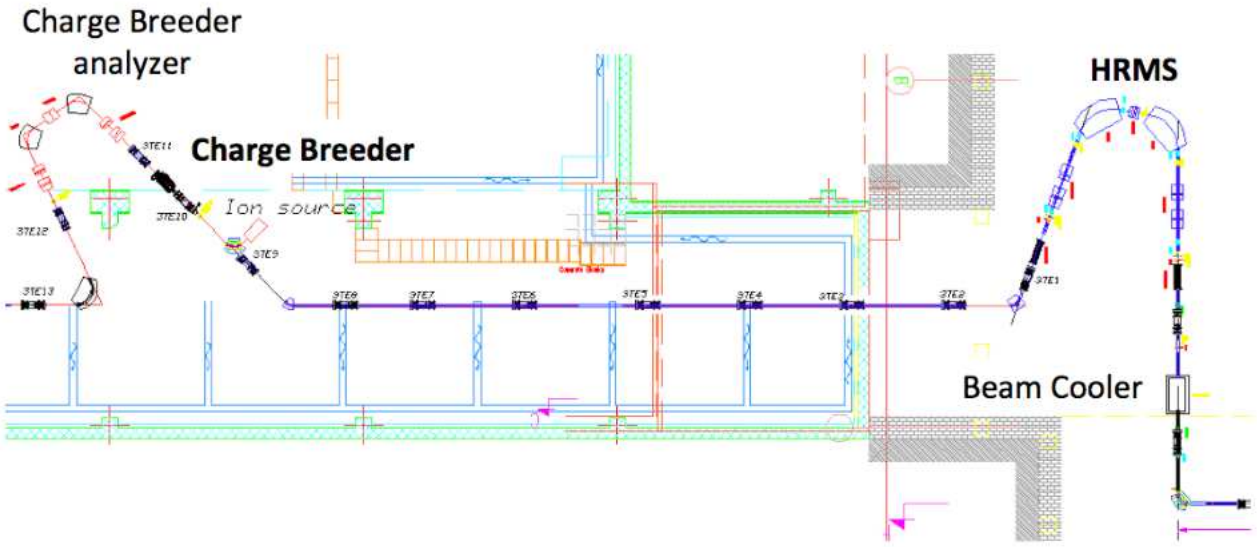

Figure 7.6: *Updated layout of the beam transport line, from HRMS to the Charge Breeder*

For sake of simplicity the description the different parts of the long beam line is presented according to the following scheme:

- Beam line from the Ion source to the Beam Cooler;
- RFQ Beam Cooler;
- Optic of the HRMS;
- Beam transport from the HRMS to the Charge Breeder;

7.2 Beam line from the ion source to the Beam Cooler

The main focusing elements of the beam transport line are electrostatic quadrupoles and sextupoles, while the bending elements are magnetic dipoles. Due to the low energy of the beam the use of magnetic lens is not convenient. Moreover, the choice of electrostatic elements produce the advantage that the working voltage of the focusing elements scale linearly with the extraction voltage of the ion source and is not depending from the mass of the ion. The field of the dipole magnets has of course to be adjusted according to the energy of the beam and mass of the ion selected. The setting of the dipole magnet anyway is greatly simplified because the right value is quite simply to be set looking at the position of the beam along the beam line.

According to the request of the RFQ accelerator the energy of the beam along all this beam transport line is 40 keV. The results here presented are been evaluated assuming a reference mass of 132 amu and a geometrical beam emittance value of 39 π mm.mrad (equivalent to a normalized emittance of 0.031 π mm.mrad)

The first part of the beam transport line consists of a quadrupole triplet T1 and by the Wien Filter WF, see fig. 7.7). The goal of this part of beam line is to perform a preliminary and a roughly mass purification with resolving power of about 1/100. Despite this poor mass resolving power, the system allow to stop at the level of the analysing collimator almost the 90% of the contaminant radioactive species coming out from the ion source. This solution allows minimize the amount of radioactivity outside the production area.

In fig. 7.8) the expected beam resolving mass is presented, while in fig. 7.9) a mass spectra obtained with the experimental set-up, already in operation, is also shown.

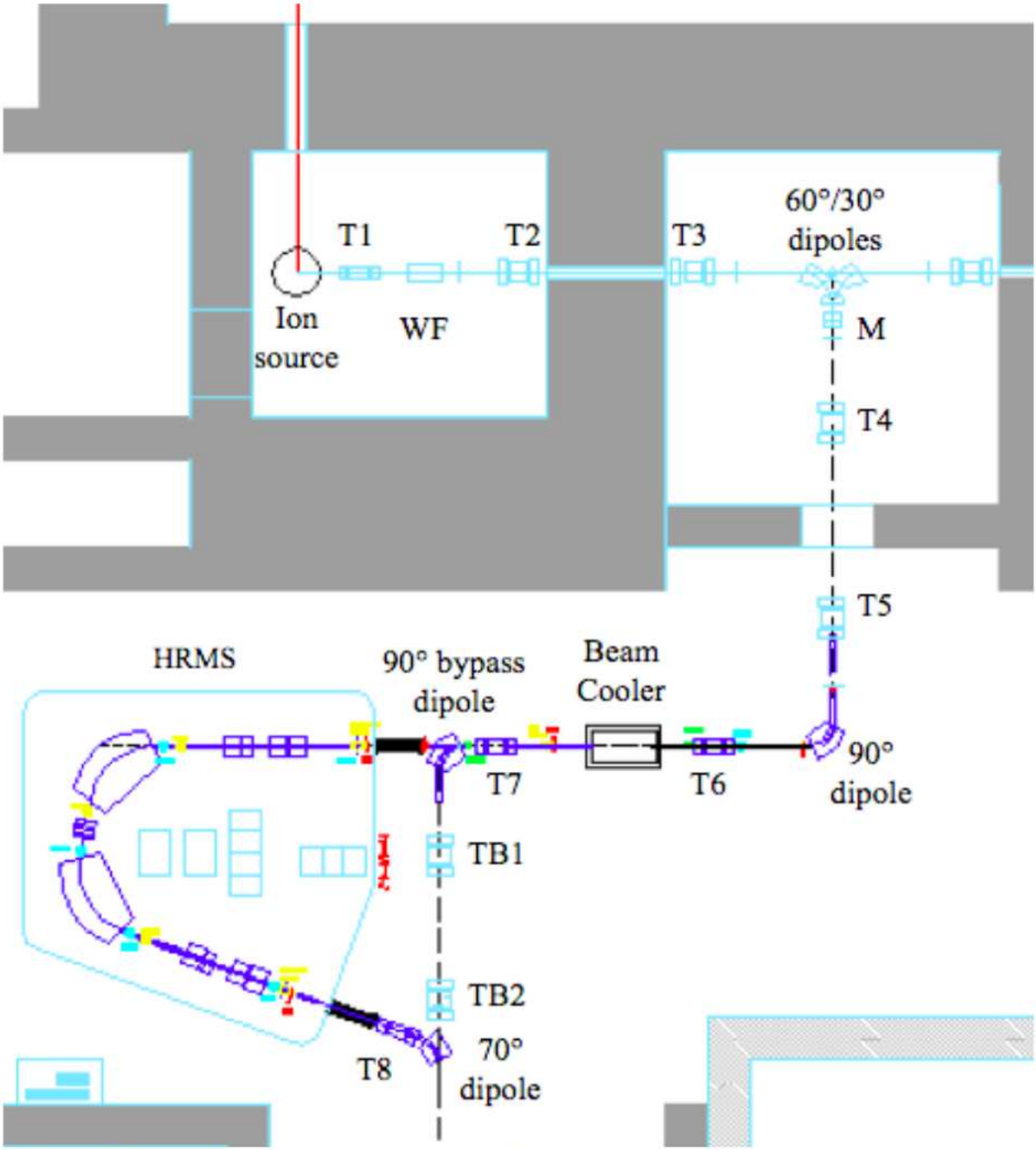

Figure 7.7: *The updated beam transport from the ion source up to the exit of the HRMS.*

The main parameters of the first triplet and of the Wien filter are presented in table 7.1. The separation gap among the electrodes of the three quadrupoles is 40 mm.

The mass resolving power shown in fig.7.8 was evaluated using the code GIOS at IIIrd order. According to the usual convention GIOS assume that the WIEN Filter has a focusing effect on the beam median plane (the symmetry plane of the magnetic field).

The quadrupole triplet T1 is used mainly to focus the beam at the selection slit placed about 40 cm after the end of the Wien filter and to compensate for the different focusing effect of the Wien Filter and for the different drift length between the virtual source position and the beginning of T1. Indeed, this distance could changes in the range 760 – 860 mm, due to different kind of ion source used.

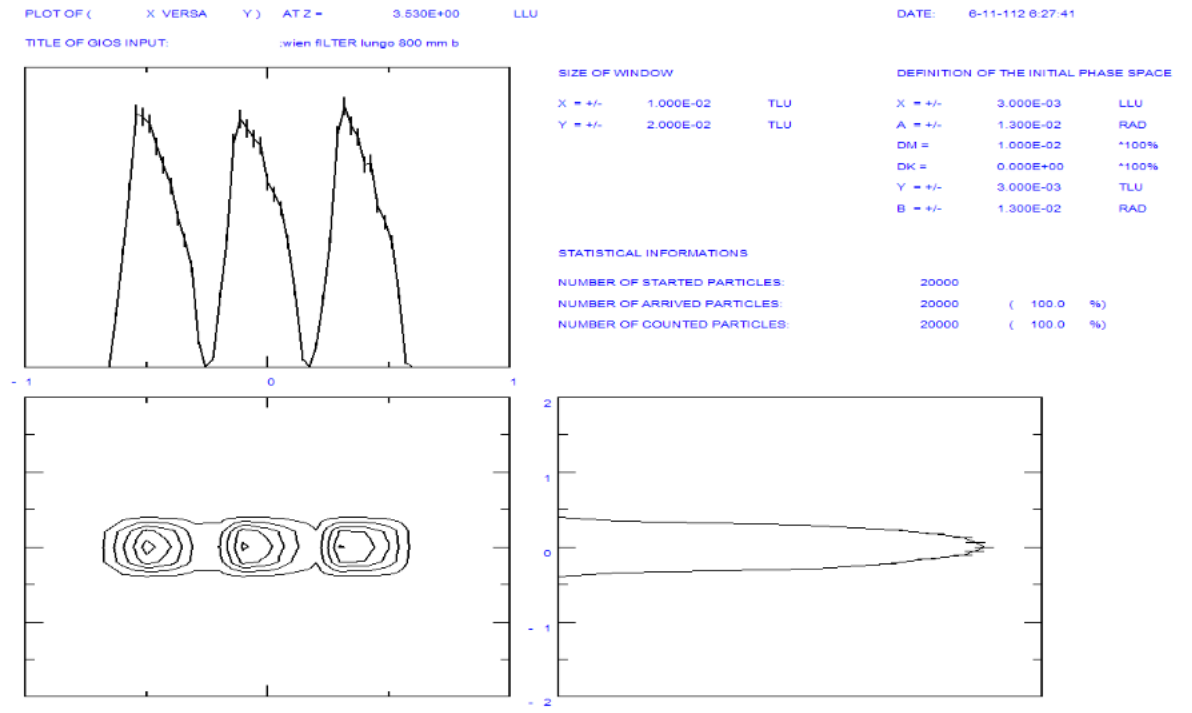

Figure 7.8: *Mass resolving power at the selection slits after the Wien Filter.*

According to GIOS code, to minimize the beam spot at the analysing slit after the WF the triplet T1 has to be sett in the configuration FDD in the radial plane, while without the Wien filter effect, or for low electric/magnetic field of the WF, the best beam focusing conditions are achieved for a setting configuration FDF. We believe that the second configuration (FDF) could be used ever, indeed we checked that integrating the orbit trajectories across the Wien Filter these trajectories have no significant difference, none additional focusing effect was detected. We have an explanation for the historical reasons that induced many authors to develop and use the wrong matrix transport of the Wien Filter, but this is outside the scope of the present report and here is not described.

Here we present the main elements of the beam transport line:

- Ion Source, this could be of different kind and has different size, see section 6;
- Electrostatic quadrupole triplet T1;
- First block of diagnostic and steerers ;
- Wien filter WF;
- electrostatic quadrupole triplet T2 before the shielding wall;
- Steerers and drift through the shielding wall;

Table 7.1: *Main characteristics of the electrostatic quadrupole triplet T1 and Wien Filter*

Name	Length (mm)	Inner diameter (mm)	Maximum Voltage
Quadrupole 1/T1	170	120	3 kV
Quadrupole 2/T1	480	120	3 kV
Quadrupole 3/T1	170	120	3 kV
WIEN Filter	Length (mm)	gap (mm)	Maximum Voltage
Electrodes	800	50	±5 kV
Magnetic field	800	130	8 kGauss

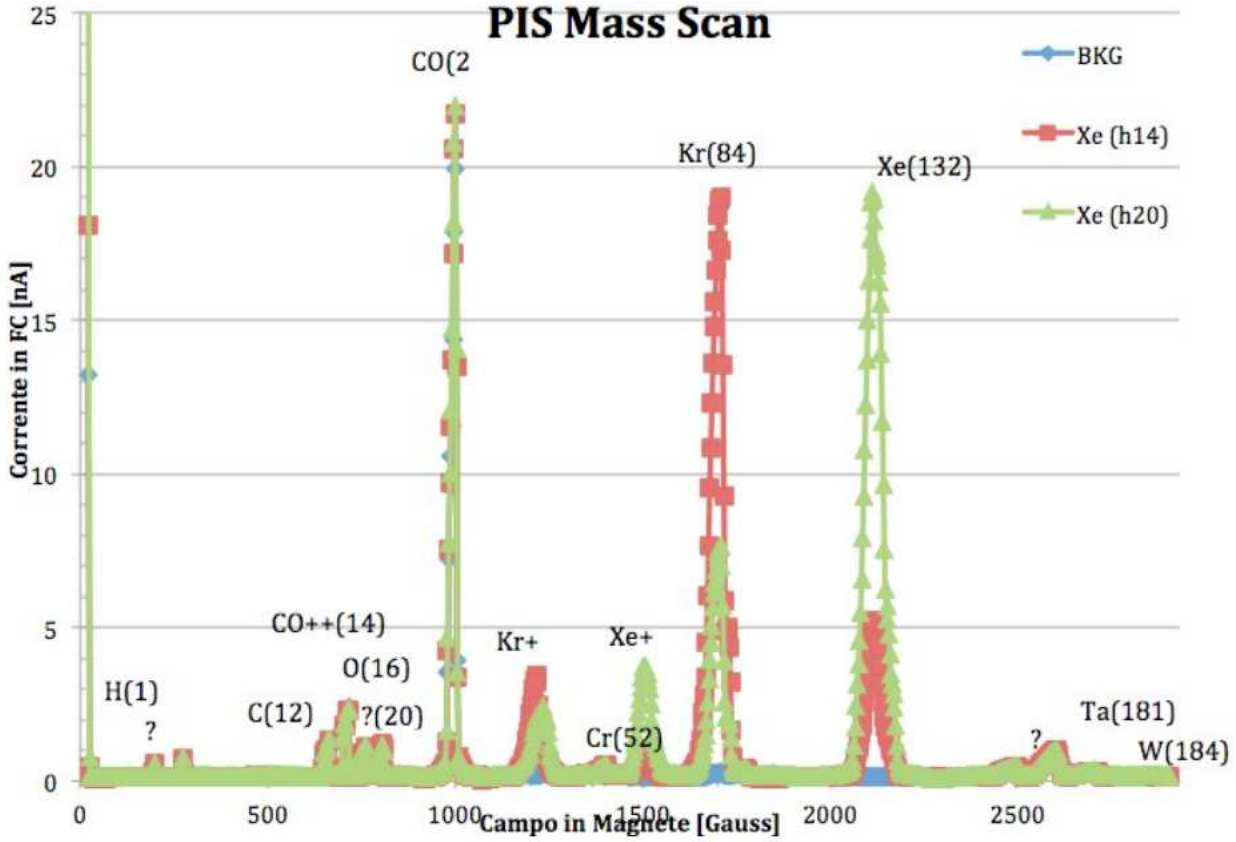

Figure 7.9: *Mass spectrum measured with the Wien Filter. The mass resolving power is not at maximum value because the electric field of the Wien filter is set at medium value.*

- Shielding wall of the production area;
- Electrostatic quadrupole triplet T3 after the shielding wall;
- Cryogenic device to stop the radioactive gas;
- 60° +30° Magnet dipoles for analysis with diagnostic blocks installed at the object and image positions;
- Electrostatic quadrupole and sextupole, to control the focalization and second order aberration at the analysis slit;
- Electrostatic quadrupole triplet T4 before the analysis shielding wall;
- shielding wall of the analysis area;
- Electrostatic quadrupole triplet T5 to focus the beam at the object point of the next analysis 90° bending magnet;
- 90° Magnet dipoles for analysis with diagnostic blocks installed at the object and image positions;
- Electrostatic quadrupole triplet T6 to focus the beam at entrance of the RFQ Beam Cooler.

In table 7.2, the drift length and the mechanical and electromagnetic characteristics of the main electromagnetic device of the transport line from the source to the analysis slit of the 60°/30° dipoles are presented. The position of the electrostatic steerers, of diagnostic box and vacuum pumps are also presented.

Table 7.2: *Mechanical and electrical parameters of the beam transport devices from source to analyzing slit of 60°/30° dipoles.*

Name	Length (mm)	Width/Heigth or diameter	Voltage or magnetic field	comments
First Drift (variabile)	760			Diagnostic+Steerers + Vacuum Pump
Quadrupole 1/1	170	φ= 120 mm	0.641 (1.9)* kV	
Drift	40			
Quadrupole 1/2	480	φ= 120 mm	-0.911 (-0.672)* kV	
Drift	40			
Quadrupole 1/3	170	φ= 120 mm	1.995 (-0.0808)* kV	
Drift	670			Diagnostic+Steerer
Wien Filter	800		5.5 kV/8 kGauss	
Drift	400			Vacuum Pump
WF Slit				x=3.2, y=25 mm
Drift	950			Diagnostic+Steerers
Quadrupole 2/1	200	φ= 80 mm	0.7126 kV	
Drift	70			
Quadrupole 2/2	400	φ= 80 mm	-0.4866 kV	
Drift	70			
Quadrupole 2/3	200	φ= 80 mm	0.4806 kV	Vacuum pump
Sextupole	150	φ= 80 mm	0 kV no necessary	Steerers
The Wall shielding	2940			Mismatch 90 mm vs. building drawing
Drift	150			
Quadrupole 3/1	200	φ= 80 mm	-0.71501 kV	
Drift	70			
Quadrupole 3/2	400	φ= 80 mm	0.50377 kV	
Drift	70			
Quadrupole 3/3	200	φ= 80 mm	-0.39914 kV	
Drift	550			Steerers
Object Slit				x=4.6, y=32 mm
Drift	1364			Cryogenic trap
Entrance edge				37.5°, R*=-870 mm
60° Dipole			10.543 kGauss	R=500 mm
Exit edge				0°, R*=968 mm
Drift	300			Vacuum pump
Entrance edge				0°, R*=30.1 mm
30° Dipole			10.543 kGauss	R=500 mm
Exit edge				0°, R*=0
Drift	125			
Quadrupole	125	φ= 80 mm	-1.354 kV	
Sestupole	125	φ= 80 mm	0.0255 kV	
Drift	400			
Analyzing slit				x=6, y=14 mm
Total length	13384			

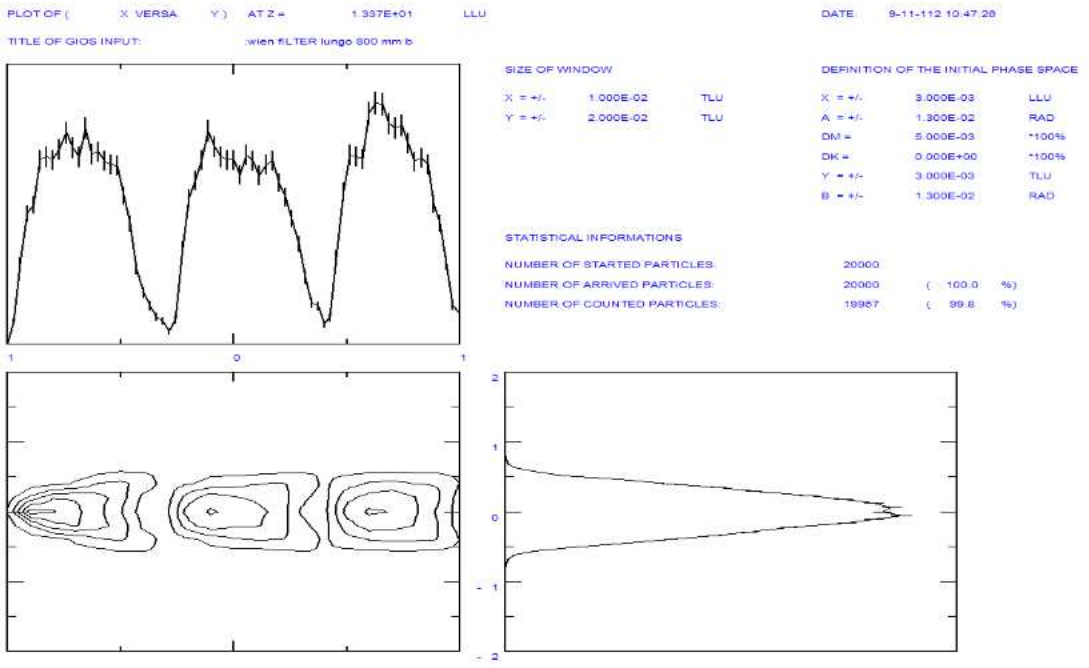

Figure 7.10: *Dispersion mass at the selection slits of 60°/30° dipole. 3rd order effects are included, mass resolving power FWtM 200. ()* These values optimize the beam envelope and the resolving mass power when GIOS code simulate the Wien Filter.*

The first drift length could change according to the different kind of ion source so also the electric voltages of the electrostatic quadrupoles of T1 could change. In table 7.2 we report the values corresponding only for the shorter drift, for the longer drift the values are a little lower. The voltages values of the electrostatic quadrupoles T1, outside the brackets are obtained assuming a free drift at the position of the Wien Filter. The voltages values for T1 put in the bracket ()*, are been obtained using the GIOS code to simulate the Wien Filter, including the radial focusing effects.

The solution to use two dipoles one of 60° and the second of 30° vs. a single double horn 90° dipoles offers some advantages:

- dipoles are smaller, this simplifies the installation;
- There is enough room (roughly 20 cm in diameter) between the two opposite 60° dipoles to install the mirror to address the laser beam to the ion source, as shown in fig. 3;
- The 3 faces entrance/exit of the two dipoles can be used to compensate the second order aberrations using proper curvatures radii.

The fig. 7.10) shows the positions of three different masses at the selection plane after the 60°/30° analysing system. The mass differences are 1/200, and the peaks are very well separated so we have a mass resolving power of 200 FWtM.

In Table 7.3, the drift lengths and the mechanical and electromagnetic characteristics of the main electromagnetic devices of the transport line, from the analysing slit of the 60°/30° dipoles to the entrance of the RFQ Beam Cooler, are presented.

In fig. 7.11) the beam envelopes in the radial and vertical plane are shown. The vertical and radial beam envelope scales are +-30 mm.

Fig. 7.12) shows the beam positions of the central mass at the selection plane after the 90° analysing system placed before the RFQ Beam Cooler. The contaminants have a mass difference of 0.350% ($\Delta M/M=1/285$). Despite the contaminant peaks are quite far from the central peak,

unfortunately these peaks are very broad so we have a contamination of about 10%. The mass mass resolving power at this slit position is 285 FWtM.

Table 7.3: *mechanical and electrical parameters of the beam transport devices from analyzing slit of 60°/30° dipoles to Beam Cooler entrance.*

Name	Length (mm)	Width/Heigth or diameter (mm)	Voltage or magnetic field	comments
analyzing slit				x=6, y=14 mm M/DM=364
Drift	1500			Vacuum pump
Quadrupole 4/1	200	120	-1.39456 kV	
Drift	70			
Quadrupole 4/2	400	120	1.14444 kV	
Drift	70			
Quadrupole 4/3	200	120	-1.39456 kV	
Drift	1400			Vacuum pump
Drift	2200			Diagnostic
Quadrupole 5/1	200	120	-1.367 kV	
Drift	70			
Quadrupole 5/2	400	120	1.23609 kV	
Drift	70			
Quadrupole 5/3	200	120	-1.367 kV	
Drift	1150			Diagnostic+
Drift	900			Vacuum pump
Entrance edge				26.5°
60° Dipole			10.543 kGauss	90°, R=500 mm
Exit edge				26.5°
Drift	1000			Ist order x=7, y=8.8 mm
Drift	990			
Quadrupole 6/1	200	120	1.3611 kV	
Drift	70			
Quadrupole 6/2	400	120	2.4205 kV	
Drift	70			
Quadrupole 6/3	200	120	-1.43037 kV	
Drift	570			
Partial length	13315 mm			
Total length from the ion source	26700 mm (26600 mm)			

After the selection slit there is just the T6 quadrupole triplet used to match the beam to the RFQ Beam Cooler. The study of the Beam cooler is in progress, so this part of matching line is not yet completed. Probably we have to replace this T6 triplet with a quadruplet to have more flexibility to match the beam cooler request.

The beam transport line could be operated or with the HRMS or trough the by-pass line. The beam line transport through the by-pass line has not yet studied. We have to solve the problem to minimize the insertion of additional quadrupoles triplet and also to avoid the mount/dismount of many components. We plan to move the two triplet T6 and T7 before and after the RFQ beam cooler to optimize the optic of the bypass line. In fig. 6) the positions of the

T6 and T7 triplet for the configuration with the RFQ in operation are shown. When we will use the by-pass line the

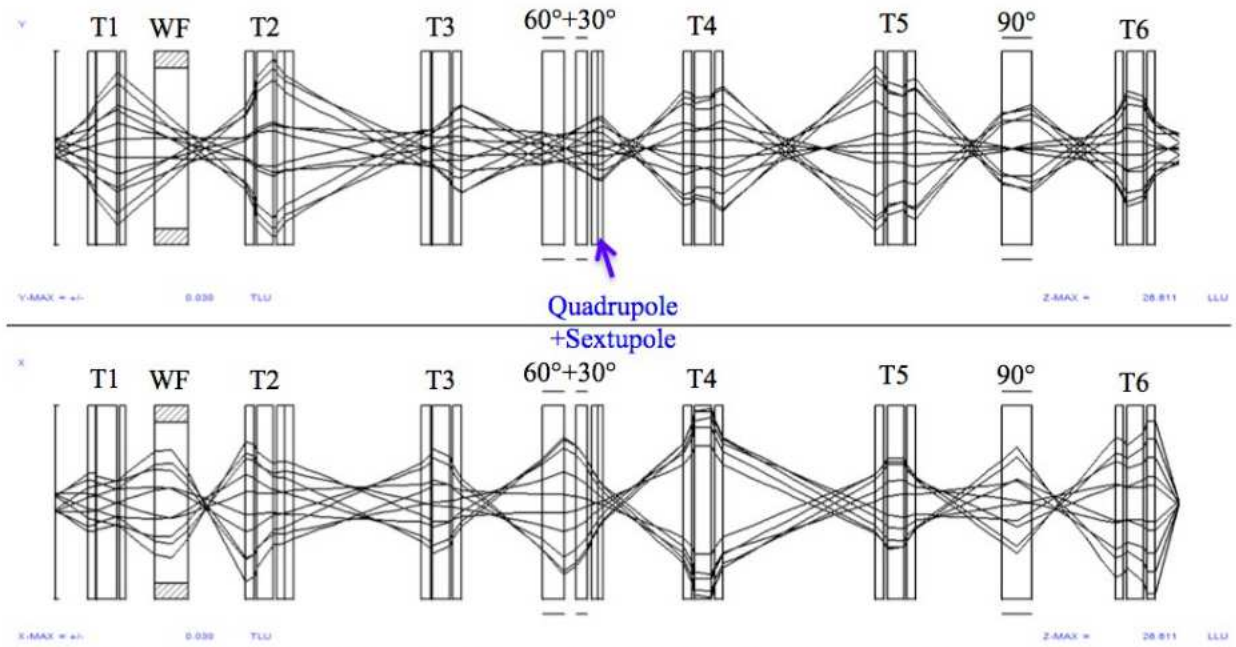

Figure 7.11: *Vertical and radial beam envelope, from the ion source up to the entrance of the RFQ Beam Cooler. 3rd order effects are included.*

RFQ beam cooler will not be in yet installed and then the two triplets T6 and T7 positions can be optimized, T6 ahead and T7 in back direction, to reduce their distance and increase the mass purification effect of the 90° dipole of the by-pass line. Working is in progress on this section, so we cannot describe further details.

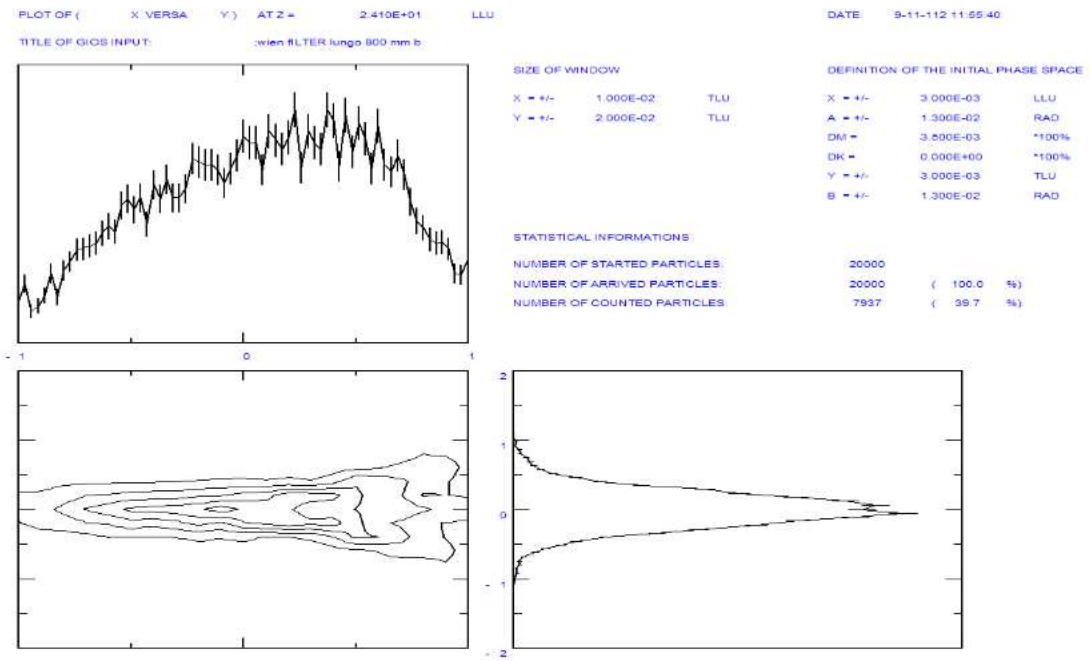

Figure 7.12: *Dispersion mass at the selection slits of 90° dipole. 3rd order effects are included, mass resolving power FWtM 285.*

7.3 Progress on the RFQ Beam Cooler Design

The experiments with radioactive beams require beams of high purity while the methodology ISOL (Isotope On LIne), used to produce them is isotopically unselective. Actually the output beam from the first mass selection (1/200) is constituted by all the radioisotopes with charge +1 and with the same number of mass. Then the radioisotope of interest have to be isolated from contaminants, which may be in the beam in quantities of orders of magnitude higher. This mass selection is carried out by High Resolution Spectrometers (HRS) whose capacity of selection (1/20000), without loss of transmission, depends on the emittance of the incoming beam. A lower emittance has the further advantage of reducing the beam transport losses and, moreover, makes easier the detection of radioisotopes and increases the accuracy of the measurement of their properties.

The devices used to reduce the emittance of low energy (a few tens of keV) radioactive beams are called buffer gas-filled Radio Frequency Quadrupoles (RFQ) cooler [2]. Many devices of this type have been successfully used up to now to reduce the beam emittance of low current (a few pnA) ion beams. However, the increased beam current intensity (up to 1μA) of the new generation ISOL facilities such as for example SPIRAL2, asks for new technological challenges for their fulfilment [3,4].

An R&D program is going on in parallel with the preliminary RFQ cooler electromagnetic and electrodynamics design in the frame of the INFN-CNV with the REGATA (2010-2012) and COOLBEAM (2013-2016) experiments.

7.3.1 Beam Cooler Concept

Insert In a RFQ cooler, a quadrupolar electric field, generated by two pairs of electrodes placed at distance $2r_o$, oscillating in phase opposition at frequency ω/2π and at amplitude voltage V_{rf}, provides a potential well which can confine the motion of a particle of charge e and mass m. It can be shown that the particle motion is stable when the Mathieu parameter q, given by:

$$q = \frac{4eV_{rf}}{m\omega^2 r_0^2} \tag{7.1}$$

satisfies the conditions $0< q<1$.

For q values included in this range, the particle motion in the quadrupole is, in first approximation, the sum of two predominant motions, the micromotion, which is the particle oscillation at the frequency of applied electric field, and the macromotion, which is due to the effect of the potential well created by the quadrupolar RF field configuration. The particle oscillation due to the micromotion occurs at the same frequency as the pilot RF field. Its amplitude is attenuated approaching the axis of the quadrupole, according to the decrease of the electric field. It is instead again amplified when the ion moves away from the axis. This type of motion is always revitalized by the electric field applied to the electrodes.

As a first approximation (for values of q less than 0.5), the frequency of the macromotion is related to that of the micromotion by the relation

$$\omega_M = \frac{q}{2\sqrt{2}}\omega \tag{7.2}$$

It may likewise be shown that, the amplitude of oscillation of the macromotion exceeds of a factor $2/q$ the maximum micromotion amplitude. The ion then performs a wide oscillations at macromotion frequency, that are perturbed by micromotion. The amplitude of the macromotion movement reduces in presence of dissipative processes, as collision with gas molecules present in the RFQ structure. The ion exchanges part of its energy with the gas molecule in the impact. It can be shown that, in average, the ion losses energy only if the gas molecule has an atomic

weight lower than the ion ones [5]. It is also important that the buffer gas is neutral and inert in order to not remove beam ions by chemical or charge exchange processes. The energy loss increases with the number of collisions, which is proportional to gas pressure. A gas inlet in the structure makes the process more efficient. The overall effect of the collisions is to introduce a viscous force which slows the ion until it reaches a constant drift speed. The introduction of this force in the equation of motion reduces the amplitude and lowers the frequency of the macromotion oscillation. The effect of the gas is therefore to reduce both transverse size and speed of the beam so to decrease its transverse emittance.

The component of the viscous force along the axis of the structure also produces a decrease in the longitudinal component of the ion speed and then lowers, together with it, also the longitudinal emittance.

To guide the beam to the exit and, if required, to allow beam bunching, a longitudinal electric field is created. The beam cooling can be carried out only when the impinging beam energy is sufficiently low to allow both the beam trapping in the potential well created by the RF field and a sufficient number of interactions between the beam ions and the buffer gas. For this reason an RFQ cooler for an ISOL facility foresees an entrance section for beam deceleration down to energy of about 100-200eV, limit given by the necessity to penetrate the potential well. An exit section makes the beam to recover the original energy.

High buffer gas pressure (up to few Pa) in the quadrupole makes the beam dumping faster but, in order not to lose beam intensity, high vacuum conditions have instead to be assured at quadrupole injection and extraction sections. Therefore, it is mandatory to maintain high differential vacuum conditions between the three cooler sections. At high beam intensities, high RF voltage amplitude (up to some kV) and, related by the *q* formula, also high frequencies (tens of MHz), are required in order to compensate for the spatial charge effects.

7.3.2 Requirements for the Spes Beam Cooler

SPES is an ISOL radioactive beam facility under construction at LNL [6]. The radioactive beam produced by the target station [7] can be re-accelerated by ALPI, the superconducting linac for heavy ions in operation at LNL, to reach an energy exceeding 10 MeV/A. SPES production facility foresees a cyclotron accelerating 700 μA proton beam up to 70 MeV. As primary beam. The impingement of the primary beam on the original production UCx target, developed at LNL, provides radioactive ions with a current intensity up to 2 μA in the mass range of 9-160 AMU. The target station is placed on a 40 kV platform. A Wien Filter located downstream the source makes a first stage mass selection and reduces the beam intensity to about 50 nA. The ion beam is then delivered through the transport line with an emittance of 30 π mm mrad at 40 kV. To improve the resolving power of the HRMS more than 1/20000, the Cooler device, placed upstream the mass selection, has to reduce the transverse beam emittance of about a factor 8. Once the beam is selected in mass, it is injected into the Charge Breeder (CB) [8] based on a ECRIS design, in order to increase the mass to charge ratio up to A/Q=7. To get the maximum injection efficiency of the CB, it is crucial to keep below some eV the energy spread of the ion beam.

The main goal of a Beam Cooler is therefore both to reduce the transverse emittance of the radioactive ion beam by a factor 8 and to maintain low the longitudinal emittance providing an energy spread of the cooled beams to about 1eV.

7.3.3 Preliminary Cooler Design

The RFQ beam cooler device is composed by 3 main sections: the deceleration system (see

fig. 1), which provides the reduction on the energy of the incoming beam from 40 keV to some hundreds of eV; the confinement and cooling section which consists on the RFQ device and the main vacuum tank placed on a 40 kV high voltage platform; finally the acceleration section where the cooled beam is extracted and achieves the initial energy of 40 keV. Buffer gas is injected in the cooling section in order to get a pressure within 0.5÷3 Pa

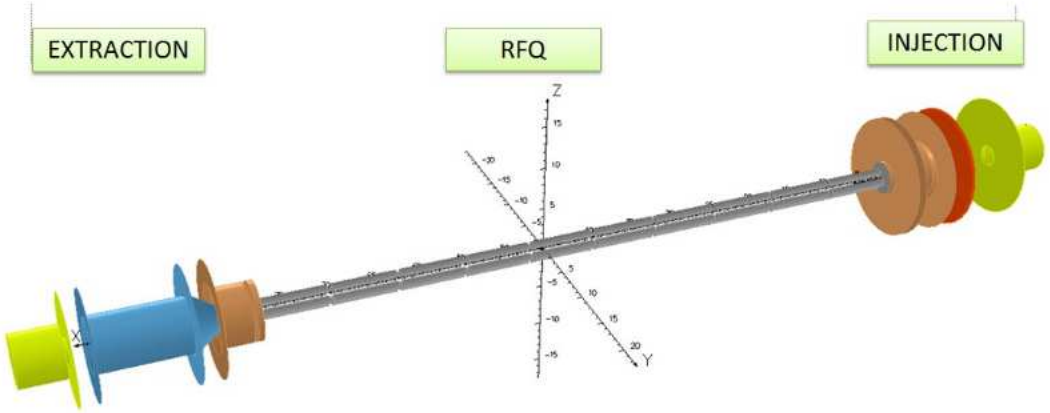

Figure 7.13: *the layout shows the main scheme of the beam cooler device. It consists of the different sections highlighted in the picture.*

The electromagnetic field configuration was studied by the use of 3D FEM code OPERA, whereas the beam dynamic was analyzed by the dedicated code SIMION ver 8 in order to take into account the collisional effects with the buffer gas molecules for simulating the cooling process. In this preliminary design phase, we neglected the space charge effects on the beam transport since the current of the Radioactive Ion Beams is lower than 100 nA.

Table 7.4 sums up the main parameters of the device.

Table 7.4 *Design parameters of a beam cooler for SPES*

Parameter	**Value**
Mass Range	9-200 AMU
Buffer Gas	He @ 293 K
Transverse Emittance injected beam	30 π mm mrad @ 40 keV (Q=1+)
Beam current	50-100 nA (10^{11} pps)
Emittance reduction factor	10 (max)
Energy Spread	< 1 eV
RF frequency range	1-30 MHz
RF Voltage range	0.5-2.5 kV
RFQ gap radius (r_o)	4 mm
RFQ total length	700 mm
Pressure Buffer Gas	0.1 – 2.5 Pa
Ion energy at cooling	100 – 200 eV

7.3.4 Injection and Extraction Sections

SPES target station delivers radioactive beams with charge Q=1+ and energy of 40 keV at the entrance of the RFQ Beam Cooler device**.** A system of four electrostatic lens decelerates the beam to 200 eV before the RFQ cooling section. The lens array gradually decelerates the ion beams to low energy, thus avoiding strong ion-optical effect that leads to harmful beam losses during the injection into the collisional ion guide.

The conical shape of the two mid stage electrodes allows beam focusing and compensates the natural diverging effect due to the deceleration process. We chose such electrode configuration in order to achieve the 100 % transmission efficiency between the injection and the RFQ sections (see fig. 2). Following the cooling process through the RFQ, the ion beams exit through a 6 mm diameter aperture and then they recovered the initial energy by a two electrode stages (see fig. 3).

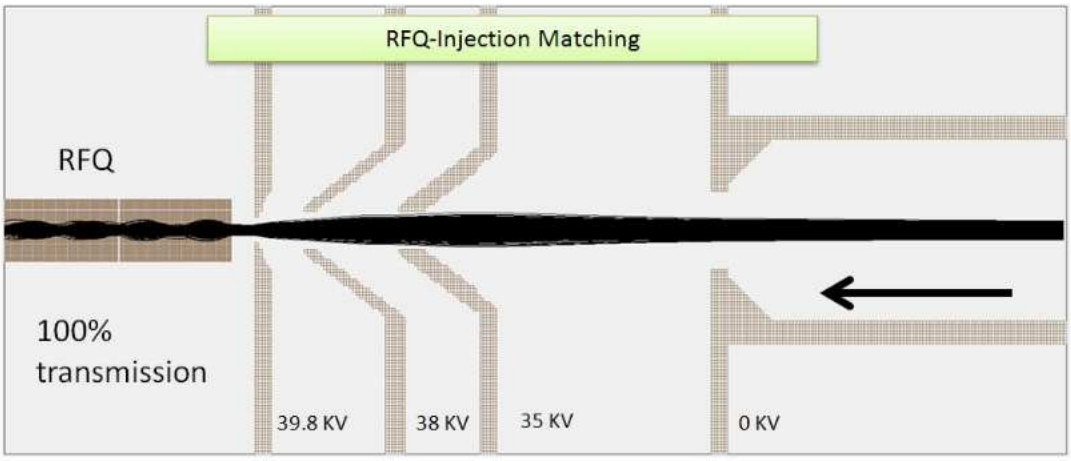

Figure 7.14: *The SIMION beam transport simulation for the $^{133}Cs^{1+}$ beam along the deceleration system. This is composed by 4 stage of electrodes at different voltage. As shown the waist is placed as close as possible to the RFQ entrance in order to fully match the related acceptance.*

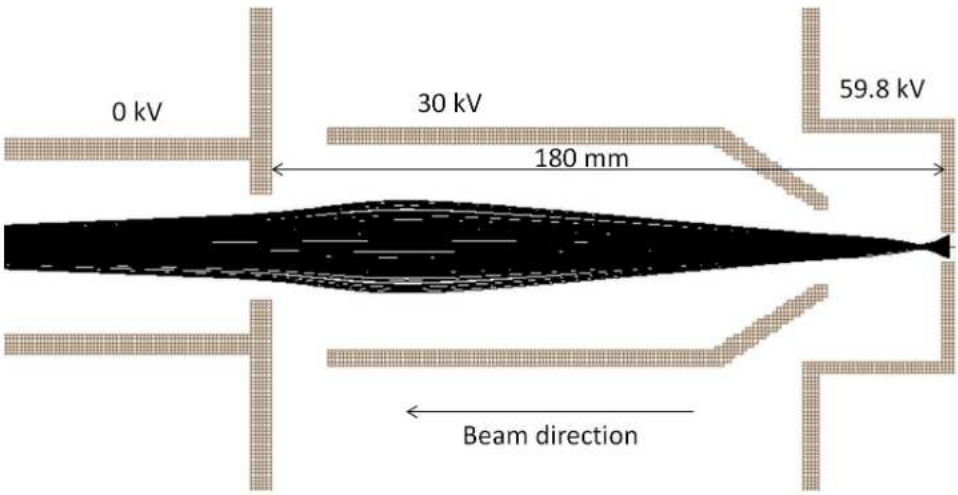

Figure 7.15: *Preliminary layout of the extraction system of the RFQ cooler and the related beam optic. The optimization process of the electrodes is carrying on.*

7.3.5 Confinement and Cooling Section

The RF quadrupole consists of four cylindrical rods of 9 mm of diameter. The distance between the opposite pair of rods is $2r_o$=8 mm The rods are 700 mm length and they are divided into 10 segments of 69.5 mm each. The segmentation allows to produce an axial field which provides the drag force needed to bring out the cooled beam. The total voltage applied along the segmentation is 100 V. The applied RF voltage and the operating frequency depends on the ion mass delivered which varies within 9-200 AMU and on the current intensity of the incoming beam. Table 1 shows the ranges of the different parameters. He at 293 °K was chosen as buffer gas for ion cooling. The operational gas pressure varies from 0.5 to 3 Pa, depending on the ion mass of the beam and on the RF voltage applied to the quadrupole.

By the preliminary results given by the SIMION code using the hard sphere model to calculate the interaction gas-ion, we simulated the cooling process and we achieved a transverse emittance reduction of a factor 8-10 as shown in fig. 7.16.

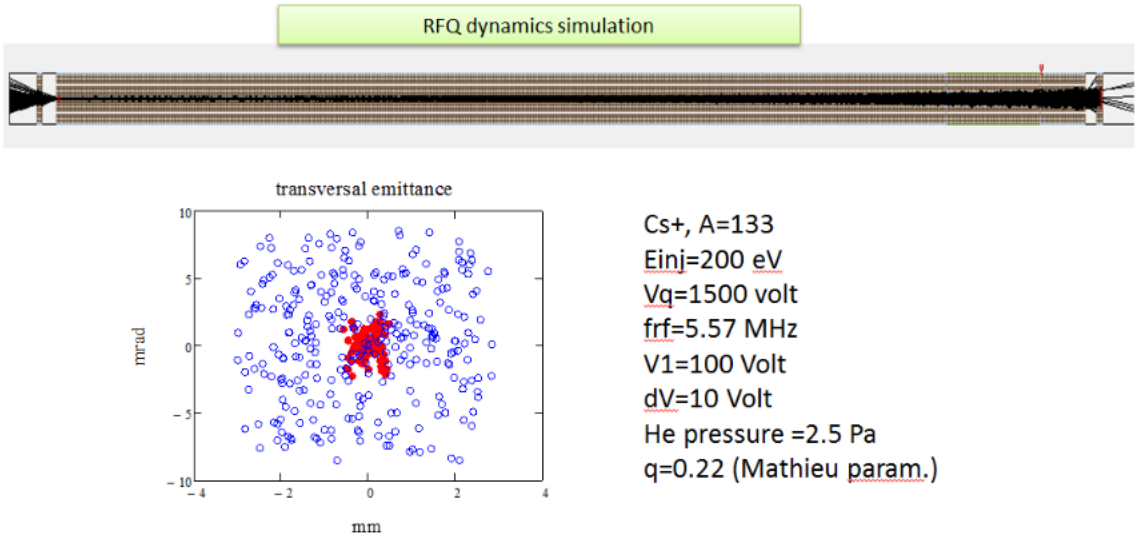

Figure 7.16: *The figure shows the simulation of the dumping of the amplitude oscillations due to the collisions of the ions with the buffer gas. The comparison between the distribution of particles on the transversal phase space at injection (blue particles) and at extraction (red particles) of the cooler device is also shown, together with the parameters of the beam and the quadrupole.*

The differential pumping system is very crucial for obtaining optimal cooling and transmission efficiency. The gas leakage through the entrance apertures causes the energy degradation of the beam and the related beam losses due to the scattering with molecules of the residual gas. These harmful effect can be reduced by both the careful design of the differential pumping system and the optimization of the design of the injection and extraction electrodes and their placing with respect to the entrance and exit of the vacuum chamber where the RFQ is placed.

7.3.6 Apparatus for discharge detecting

Despite the expected radioactive ion beam intensity for SPES (50 nA) is lower than ones reachable in the facility SPIRAL 2, however it is anyway much higher than other coolers in operation.

As described in the previous paragraph, a high current cooler requires to apply an RF voltage of some kV to the electrodes in presence of a buffer gas at pressure of some Pa.

This pressure range is near to the minimum of the Paschen curve [11], which states the discharge voltage as a function of the product between pressure and electrode distance, as a consequence electrical discharge can be an issue for the beam cooler operation. For this reason we foresaw, in the frame of the experiment REGATA, the construction of an experimental set up aimed to experimentally study the conditions at which the discharges between the electrodes may occur. In such apparatus we can assemble electrodes of different shape and automatically vary their distance without the necessity to open the vacuum chamber. In addition we can easily change the applied (DC) voltage or Helium pressure level. In such way we can evaluate the dependence of the discharge offset from such parameters and, moreover, the influence of shape and surface preparation of electrodes.

The test apparatus includes a CF150 flange (fig 5) which holds the two electrodes. One of the electrode, supported by PEEK made insulators is connected by an high voltage feed-through to a high voltage power supply. A linear actuator allows to change the position of the second electrode, maintained at ground potential. The assembling system is designed in order to make an easy exchange and alignment of electrodes. The CF flange has apertures for the pressure gauge and gas inlet and will be integrated in an existing high vacuum apparatus. Figure 3 presents the working scheme of the test discharge apparatus and of its control system.

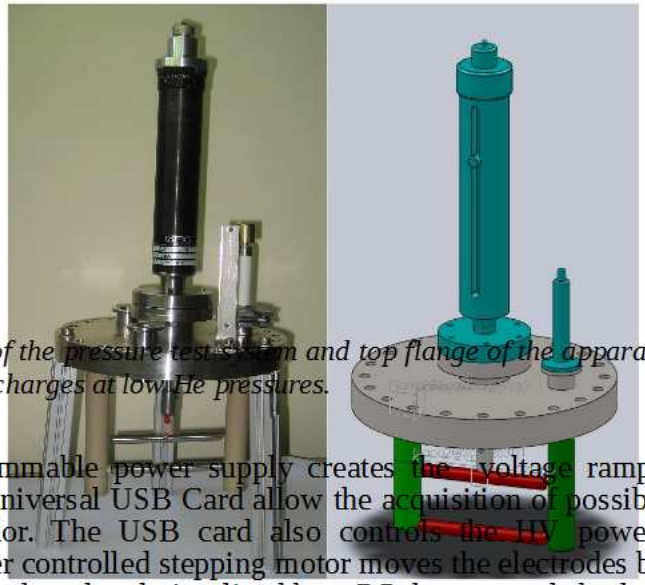

Figure 7.17: *Drawing of the pressure test system and top flange of the apparatus under construction for testing conditions of discharges at low He pressures.*

A 10 kV programmable power supply creates the voltage ramps. Both a four channel oscilloscope and an universal USB Card allow the acquisition of possible current spikes and of their dynamic behavior. The USB card also controls the HV power supply and gas flow equipment. A computer controlled stepping motor moves the electrodes by a linear feed-trough.

All the data are gathered and visualized by a PC that controls both electrode movement and test operation sequence.

Figure 7.18: *Working scheme of the test set up for detecting discharges at low gas pressure*

7.4 High Resolution Mass Separator

The goal of SPES project is to provide to the LNL users radioactive beams having mass between 20 and 180 amu. Unfortunately, in this mass range nuclei that have the same number of nucleons, but different combination of protons and neutrons number could have mass difference very small, often of the order of 1/3000.

For example the inverse of the difference of relative mass (A/ΔA) for the isobaric nuclei from Kr to Sn, which have A = 100 goes from 9200 up to 29 000 with the exception of ^{100}Mo and ^{100}Tc, virtually indistinguishable because require a separator mass with resolving power greater than 550.000! Similarly for other pairs of Nb/Ru, Rh/Zr and Y/Pd, equidistant from the valley of stability and that, all these, have a mass difference less than 1/50.000. Similarly for the isobars from Te to Ho that have mass A=140, the difference of relative mass (A/ΔA) varies from 11.500 up to 38.500 with the exception of ^{140}Ba and ^{140}La virtually indistinguishable because they require a separator with a mass resolving power greater than 348 000! Also for the other pairs of nuclei equidistant from the valley of stability. However, As the pairs of nuclei are far from the stability valley, the difference in their mass increases, see fig. 7.19). This critical situation is attenuated when the mass of nuclei decrease, for example in the case of isobaric nuclei with A=50, ranging from Cl to the Ni the A/ΔA vary from 2100 to 21000 with the exception of the couple of ^{50}Cr/^{50}Mn which has A/ΔA= 44800. The mass values used in the present calculations are from [12].

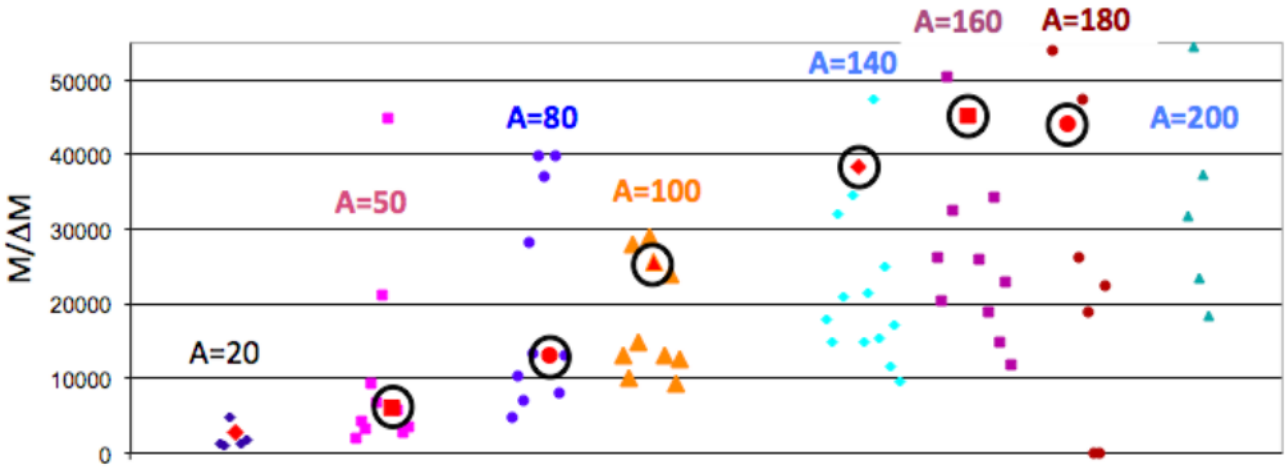

Figure 7.19: *A selection of mass resolving power necessary to distinguish 2 contiguous isobars, for different mass groups. The dots of different colour of each series and circled correspond to contiguous isobars at center of stability valley. For the heaviest group a lot of contiguous isobars have mass/ mass differences (M/ΔM) ratio exceeding the scale of the figure.*

Fortunately, the smaller values of the mass difference ΔM, or the Highest values of M/ ΔM, are between the couple nuclei that stay near the center of stability valley, while when we move away from the stability valley these differences increase.

Although mass spectrometers capable of measuring mass differences of 1 part in 100,000 they were already build, so far not been realized separators / purifiers with resolving power in mass greater than 24000. Indeed a mass separators or mass purifiers has to minimize the contamination of the neighbors nuclei and for this the usual definition of mass resolving power of the mass spectrometers is not a good parameter. The usual mass resolving power at the first order is defined as M16/(2X0), where M16 is the mass dispersion (equal t ½ to the momentuum dispersion when we analize a constant energy beam) and 2X0 is the Full Width half Maximum

(FWHM) of the beam. This definition means that about 50% of the two neighbors nuclei is mixed with the required nucleus.

For this reason in the following we like to adopt a definition of mass resolving power a little different than the previous M16/(XWt) were XWt is the width of the beam at 1/10 from maximum (FWtM). For a Gaussian distribution this means roughly that XWt is about double respect to the FWHM, so M16/(XWt)≈M16/(4X0).

For the SPES project, a few years ago, we set ourselves the objective of creating a separator with a resolving power in mass> 20000 based on the design of EXCYT project. Today we are confident that we can build a separator with a mass resolving power of about 40000.
The main goals of our magnetic separator is to purify the beam and at the same time to have a transmission efficiency greater than 90%, moreover a continuous operation and high level of reliability are requested too.

We decided to study a magnetic separator separator very similar to the one proposed for the project CARIBU of Argonne laboratory [13], A compact high-resolution isobar separator for the caribou project. Indeed this separator meet the needs of the SPES project.

In fact, the main features of this isobaric separator are:

- It is quite compact and has a simple design, which allows easy tuning;
- It consists just of two magnetic dipoles, while all other focusing and corrections elements are electrostatic and this means that the "setting" and the corrections are independent from the mass of the ion desired, but scale just with the energy of the beam;
- It has a mass resolving power of 22000, a transmission greater than 95%, while assuming as initial dimensions of the beam a beam spot of 1 mm and an emittance of 3 π mm.mrad and a spread energy of the beam of ± 1 eV.

This means that the beam to be analyzed must be suitably cooled in the phase space by means of a RFQ Beam Cooler, before being analyzed by HRMS. However, the initial specification of the beam seem achievable by the new generation of RFQ Beam Cooler that are being developed in several laboratories.

The solution of a magnetic separator such as proposed by T. Giles for EURISOL there seems unsatisfactory for various reasons. Such as for example, the initial size of the beam must be only 0.12 mm FWHM to obtain a momentuum resolving power of 50000, and also the use of only 4 magnetic dipoles does not allow to have enough tunable parameters to the first order, then the system is much more rigid . Moreover the correction of the higher orders aberration should be magnetic and therefore dependent on the mass of the ion. The spectrometer of Caribu project at Argonne with a beam size of just 0.4 mm may have a resolving power in mass equal to 55000!

The layout of the spectrometer we propose is shown in Fig 1) and it is composed of the following elements:

- Two magnetic dipoles with deflection angle of 80° and bending radius of 1.5 m;
- Two doublets and two singlets electrostatic quadrupoles;
- Two electrostatic sestupoles and one electrostatic multipole.

This design makes it possible to obtain a mass resolving power of about 45000, to first order assuming the definition of beam size FWtM. Using the sestupole we are able to compensate the 3rd order effects and maintain the mass resolving power value equal to 40000.

The main differences respect to the mass separator of CARIBU projects are:

- the bending radius of the two dipoles is increased from 60° up to 80°;

- the large bending radius of the dipoles 1.5 m vs. 0.5 m;
- the higher energy of the beam 260 keV vs. 50 keV;
- the initial beam size spot is 1 mm vs. 0.4 mm;

The bending radius and the bending angle were increased to achieve the resolving mass power of 40.000 FWtM.

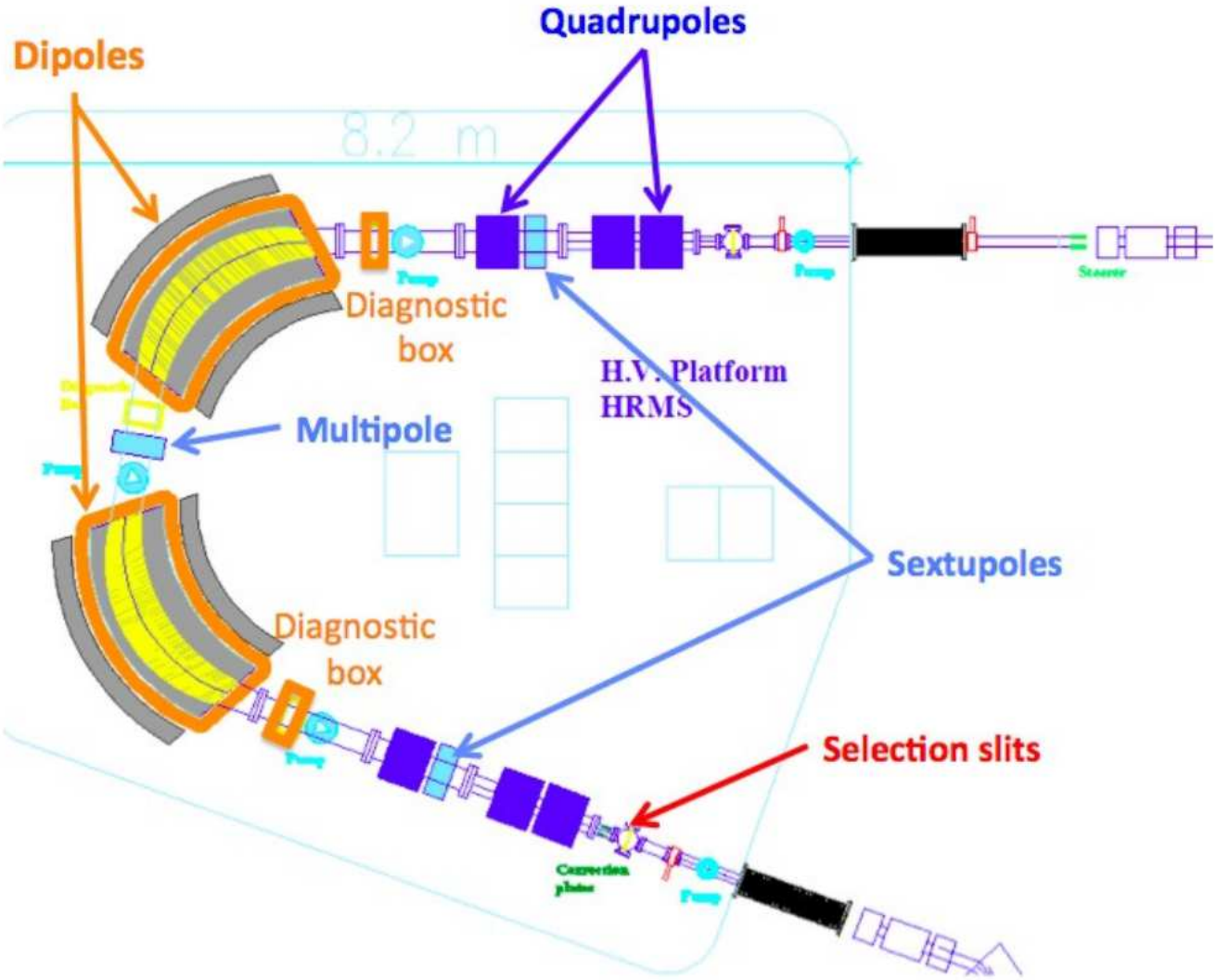

Figure 7.20*: Layout of the High Resolution Mass Separator.*

At the same time we have to increase the beam energy to maintain the minimum field of the dipole higher than 1.5 kGauss also for the lower mass of the analysed ions. According to the magnetic rigidity of the different beams the magnetic fields vary from the maximum value of 6.57 kGauss (A = 180 @ 260 keV → Bρ = 0985 Tm) to the minimum value of 1.6625 kGauss (A = 20 @ 150 keV → Bρ = 0249 Tm). The minimum value is about ¼ of the maximum value and in any case not very low.

It is important magnetic field not very low to be quite sure to achieve a good magnetic field uniformity and also a uniform scaling of the whole magnetic field at the different values of setting.

There are two further advantages to analyze beam with energy 260 keV vs. 50 keV:

- the transverse beam emittance could be larger and then the transmission efficiency higher than 95% is easier achieved;
- an energy spread of ±1 eV is acceptable.

The deterioration effects of the energy spread is quite evident looking at the fig. 7.21 a,b,c. Where the peak sizes for the energy spread of 0.5, 1 and 2.6 eV are respectively shown. To analize a beam with 260 keV we need to put HRMS on an High Voltage platform with maximum operating voltage of 220 kV. Despite this pose significantly problem we like to point out the great advantage of this solution. According to fig 7.21 c) we can see that if we have to analize a beam with energy of 100 keV an energy spread of ±1 eV is not acceptable to achieve a mass resolving power of 40000. Moreover the H.V. platform can be switched on just for the cases when the highest performances are necessary. In the first years of operations or for the ligter ions we don't need to use the H.V. platform at highest values. If low values of mass resolving power are enough the voltage of the platform can be switched off.

Of course the best performances of the HRMS strongly depends on the performances of the RFQ beam cooler. The best performances of the HRMS are achieved for a radial beam emittance of 2 π mm.mrad and for an energy spread of ± 0.5 eV, in this condition a mass resolving power up to 60.000 could be achieved selecting the beam at the entrance with slit aperture of ± 0.25 mm. Probably this could be achieved loosing somethings in term of transmission efficiency.

We like to stress that the beam emittance could depend strongly by the mass of the beam and in particular larger is the mass of the ion larger is the beam emittance. In particular ion with mass A=132 with geometrical emittance of 2 π mm.mrad correspond a very small normalized emittance of 0.004 π mm.mrad, while for mass A=50 the same geometrical emittance is equivalent at a normalized emittance of 0.007 π mm.mrad. This means that the acceptance of HRMS is higher for lighter ions.

On the other side we can increase the acceptance of the HRMS if we accept to loose in mass resolving power.

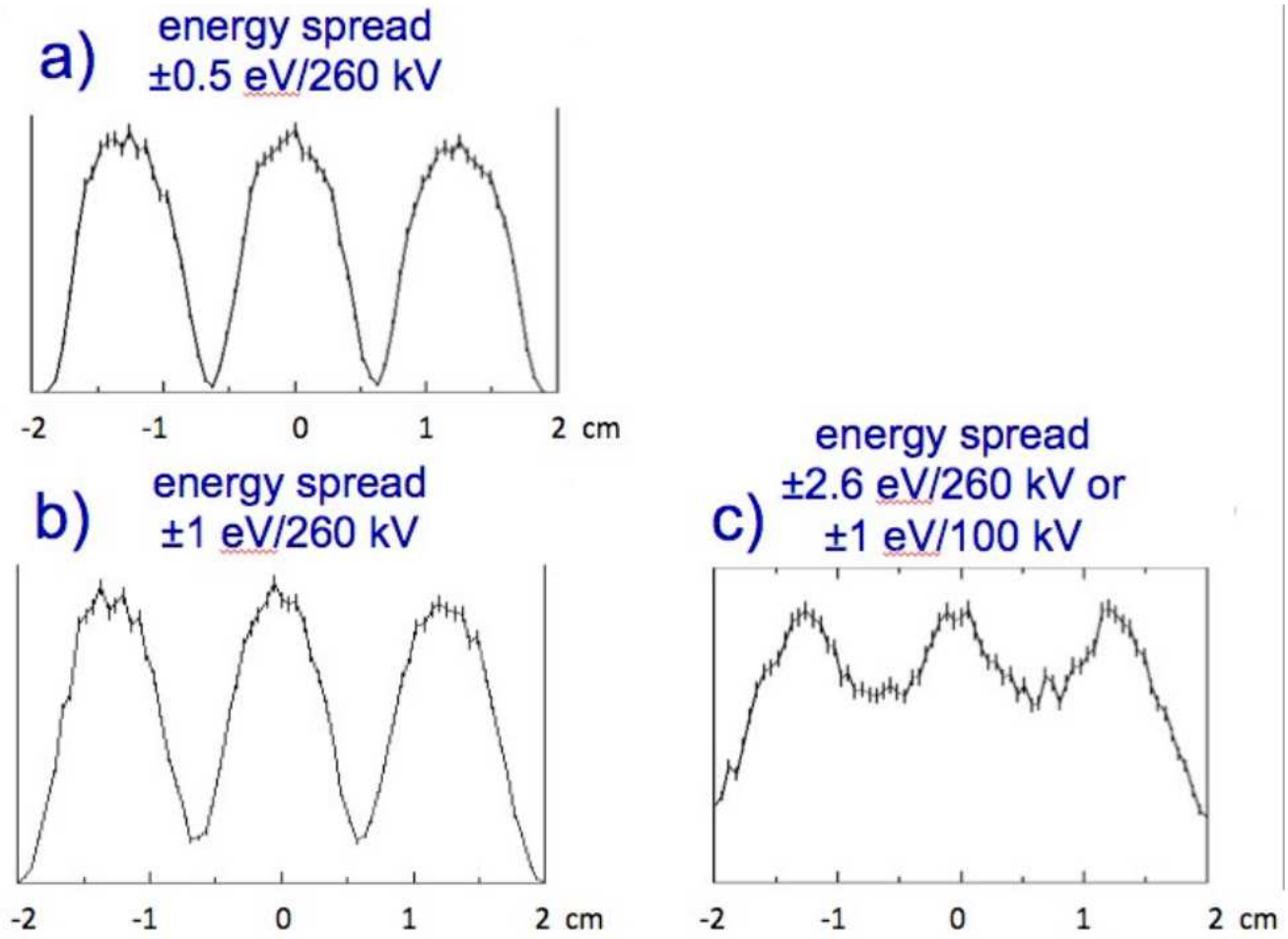

Figures 7.21 a,b,c: Energy spread decreases significantly the FWtM mass resolving power of the HRMS.

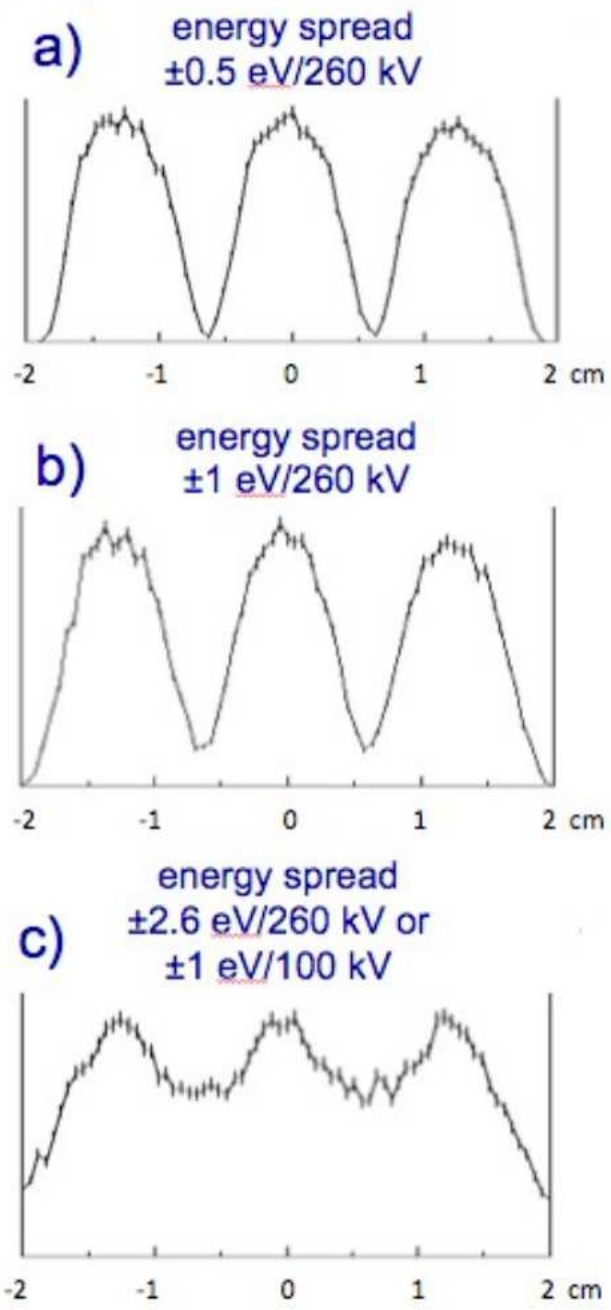

Figures 7.21 a,b,c: Energy spread decreases significantly the FWtM mass resolving power of the HRMS.

7.4.1 Optic of the HRMS

The beam envelope in the (Y, Z) and (X, Z) spaces are shown in Fig. 7.22). The maximum beam sizes of beam in the two planes are significantly different, ± 6 mm in vertical and ± 250 mm in radial. The perfect symmetry of the separator allows a reduction of the intrinsic aberrations. The beam is assumed to enter from a slit with a diameter of 1 mm and with a divergence of ± 8 mrad in both planes. The first doublet of quadrupoles realizes a transport point to point but with a nominal magnification of approximately -0.19 in the plane (X, X ') and of about -3.4 in the plane (Y, Y'). The third quadrupole, the angle of the dipole faces and the distance between this quadrupole and the dipole are chosen to achieve the conditions R_{22}, R_{34}

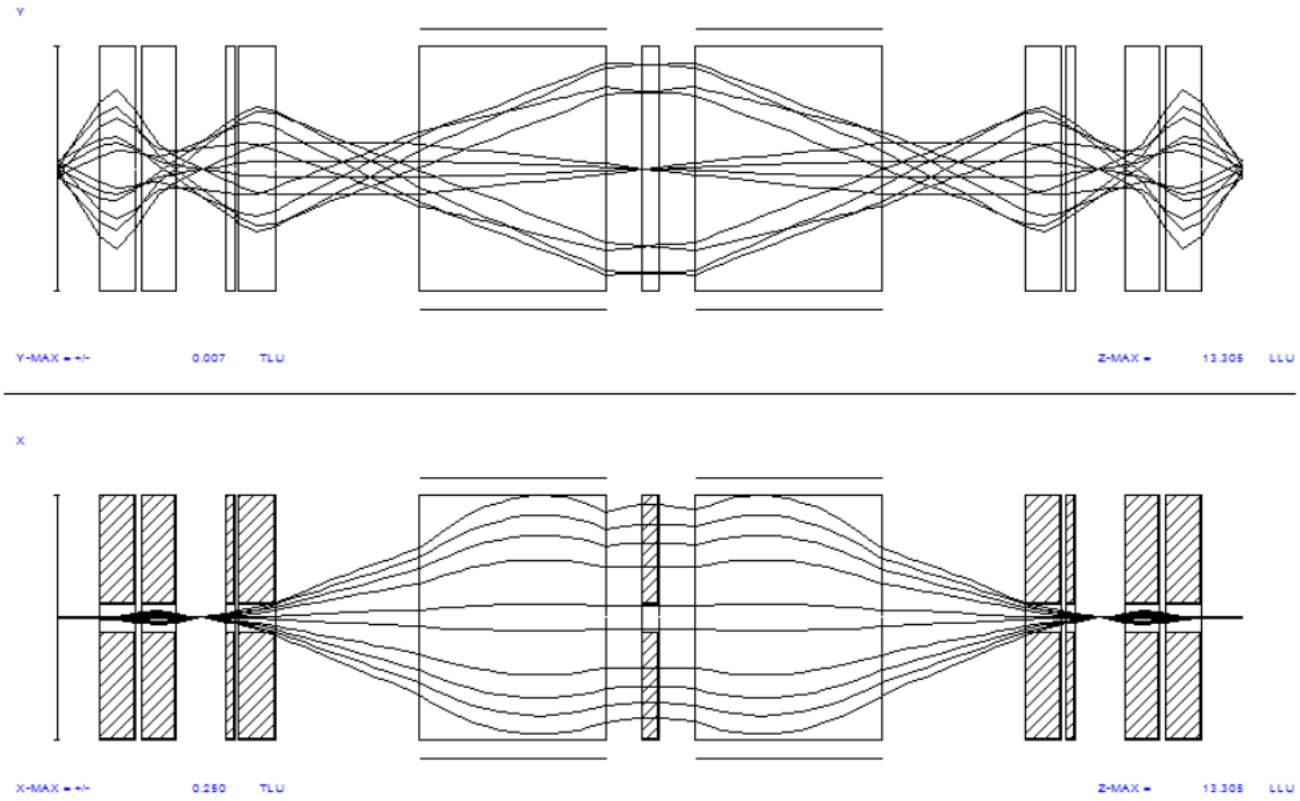

Figure 7.22: *Vertical and radial beam envelopes including the 3rd order effects.*

and R_{43} equal 0 in the symmetry plane of the system. The resolution of the system depends mainly on the radius of bending of the dipoles and also by the distance between the dipole and the third quadrupole. Instead, it is practically insensitive to the distance between the two dipoles.

Different configuration of the system were studied with bending angles from 60° to 90°. These simulation confirm that the envelope of the beam in the radial plane decreases when the bending angle increase, of course, at mass resolving power and beam emittance constant.

The design of the HRMS is now frozen and the characteristics of the system are presented in table 7.5. Further studies are necessary before to start the engineering design of the dipoles. In particular we have to optimize this design looking at the fifth order correction using the COSY infinity code and/or using raytracing code. Moreover up to now the beam emittance is quite larger than the expected beam emittance delivered by RFQ. For this reason is strongly suggest to optimize the size of the dipoles just after the RFQ beam cooler characteristics will be fixed.

Another key constraint to be analyzed is the room temperature of the HRMS and its uniformity. Indeed a temperature variation of 1 K , considering the size of separator are 8 x 8 m^2, could produce a legth variation of the separator of about 0.4 mm. Despite this value is small the position of the multipole correctors are very sensitive at these changes.

Table 7.5: *mechanical and electrical parameters of the HRMS elements.*

Name	Length (mm)	Width/Heigth or diameter (mm)	Voltage or magnetic field	comments
Object point				x=±0.5 mm, x'= 4 mrad y=±0.5 mm, y'=8 mrad
Drift	500			Diagnostic devices
Quadrupole 1	400	60	-2.38863 kV	
Drift	70			
Quadrupole 2	400	60	2.8281 kV	
Drift	530			Vacuum pump
Sextupole 1	100	60	-231.9 V	
Drift	50			
Quadrupole 3	400	60	-1.089 kV	
Drift	1621			Diagnostic devices
Entrance edge	28.357°			
80° Dipole 1	Radius bending 1500 mm	Gap <80 mm	5.623 kGauss	Radial beam size ± 140 mm vertical size ± 6 mm
Exit edge	28.357°			
Drift	450			Vacuum pump
Sextupole +Octupole	200	500 mm	Sext=9.3086 kV Oct=0.1584 kV	
Drift	450 mm			Diagnostic devices
Entrance edge	28.357°			
80° Dipole 1	Radius bending 1500 mm	Gap <80 mm	5.623 kGauss	Radial beam size ± 250 mm
Exit edge	28.357°			
Drift	1621			Diagnostic devices
Quadrupole 4	400	60	-1.089 kV	
Drift	50			
Sextupole 1	100	60	1.4070 V	
Drift	530			Vacuum pump
Quadrupole 2	400	60	2.8281 kV	
Drift	70			
Quadrupole 1	400	60	-2.38863 kV	
Drift	500			Ripple Deflector plate
Selection slits				x=±0.5 mm, x'= 4 mrad y=±0.5 mm, y'=8 mrad + Diagnostic devices

7.4.2 Compensation of H.V. platform ripple

Despite the RFQ beam cooler should delyver a beam with an intrinsic energy spread lower than ± 1 eV, anyway the beam energy is affect by an energy ripple introduced by the H.V. platform.

The platform ripple could be up to ± 5 eV and therefore might destroy the resolution of the HRMS. In fact 5 eV/250kV → ± 2 · 10-5 and this produce a displacement of the beam centroid of about ± 1 mm. Fortunately the ripple of the H.V. platform is a coerent effect and it is quite slow. Its typical frequency are harmonic of the 50 Hz of the main line. Also if we assume a 1 kHz ripple frequency the period of the ripple stay around 1 msec that is quite easy to use an active system to compensate this bad effect.

The feedback to maintain stable the position of beam centroid can be accomplished by a couple of deflection plates of 50 x 50 mm2 size and a 20 mm gap, placed after the last quadrupole and 20 cm before the analysis slit. A driven voltage of ±500 V is enough to compensate the expected ripple of ±5 eV of the H.V. platform (±2 10^{-5}).

7.5. Beam transport line from the HRMS to the Charge Breeder

From the High resolution beam spectrometer to the charge breeder is necessary to transport the beam for about 37 meters in a carefully way to avoid beam losses. This periodic line is made by using electrostatic triplets with a period of about 3.6 meters; the total length of the line so may be changed to fit future variations of HRMS or Charge Breeder positions by adding a period or removing a period.

The assumption in the calculation is an RMS normalized emittance of 0.02 mmmrad, and a total normalized emittance of 0.08 mmmrad. This beam emittance values are a little higher than the expected emittances of beams coming out from the source and assuming don't use the RFQ beam cooler.

The layout of the line is reported in fig. 7.23), while in fig.7.24) the beam envelope in the radial and vertical plane are also shown. The maximum size of beam enevelope in both planes are similar and equal at about 45 mm in radius. The technical specifications of the electrostatic quadrupoles and of the two magnetic dipoles are presented in table 7.6.

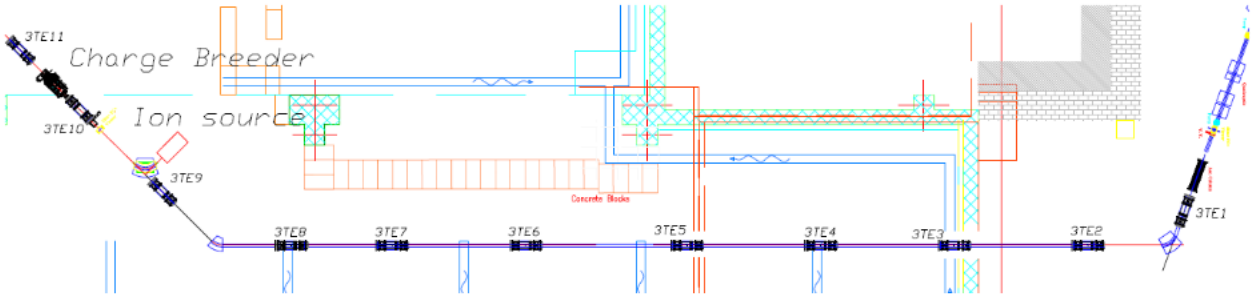

***Figure 7.23**: Layout of transport line, from the exit of the HRMS into the 3° experimental Hall.*

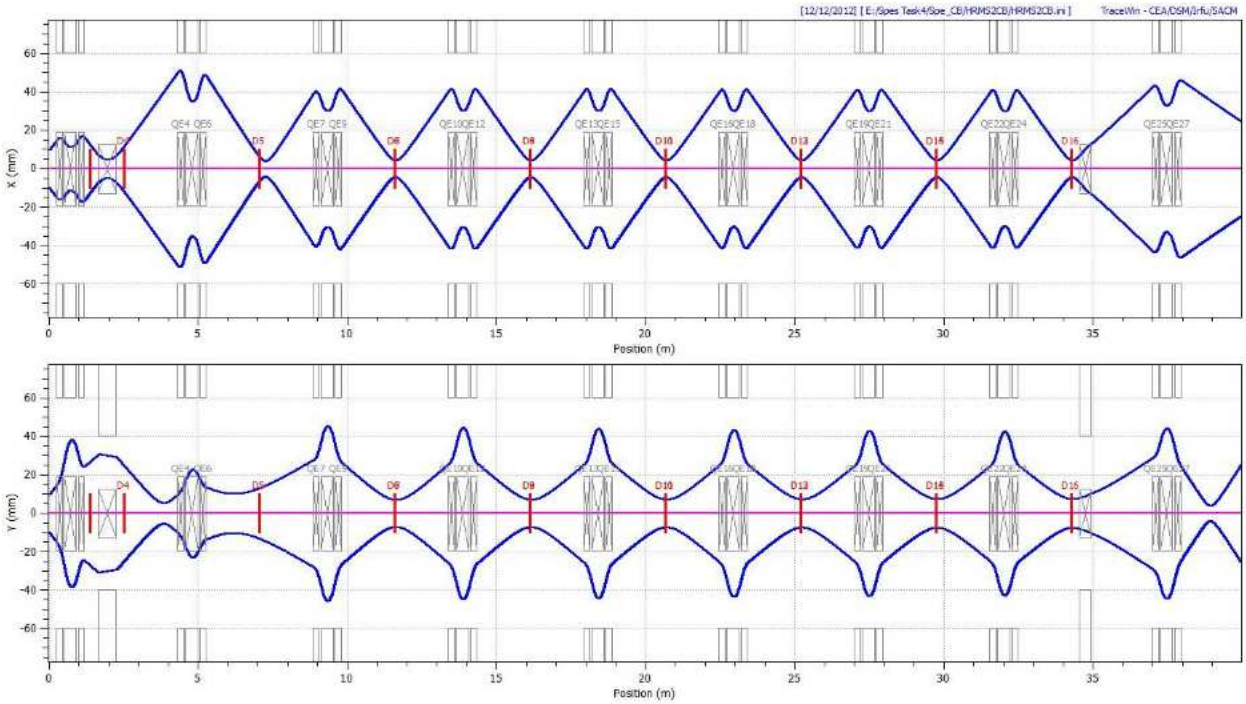

***Figure 7.24**: beam envelopes in X and Y directions along the line from the HRMS to the CB.*

***Table 7.6:** Transport line to the Charge breeder main parameters, for transport of ion with mass A=132 at 40 keV*

Ion	1/132
Electrostatic Triplet lengths (mm)	200+70+400+70+200
Electrostatic Triplet radius	60 mm
Electrostatic max voltage	4.03 kV
70° Dipole Radius	500 mm
70° Dipole max field	0.66 T
45° Dipole Radius	500 mm
45° Dipole max field	0.67 T
Energy (1/132)	40 kV
Total number of triplets	10

7.6 Low Energy beam diagnostics

A research activity has to been started in order to adapt the diagnostics developed for the EXCYT (EXotics with CYclotron and Tandem) facility working at LNS, by taking into account the specific requirements of the SPES beams, that in a few words are the higher intensities and the heavier radionuclides. Such diagnostic devices should be based on multidetectors, that allow the on-line acquisition of the beam profile and position, the beam intensity and the isotope identification.

In the following is reported a short description of the EXCYT beam diagnostic devices LEBI (Low Energy Beam Imager/Identifier) [14], installed along the low energy beam line (10 - 300 keV). Such devices are based on particle detectors and are well suited for the peculiarities of the EXCYT beams, thus ensuring quick and precise beam transport procedures. They allow to measure the main radioactive beam parameters in real time, in particular the transverse beam profile and its intensity, allowing also the identification of the radioisotopes in the beam.

Each device is mainly made of two components (fig. 7.25): one is used for beam imaging purposes and it is based on a scintillating screen (5×5 cm^2 area, 1 - 2 mm thick) of Cesium Iodide doped with Thallium, CsI(Tl), chosen since its light yield (6×10^4 photons/MeV) is far higher than the ordinarily used phosphor screens. Such a screen is placed at an angle of 45° with respect to the beam axis and is watched by a high sensitivity CCD camera (WAT 902H, sensitivity of 10^{-4} lux).

The second component is used to detect beta particles emitted as a consequence of the radioactive decay. It can measure the beam rate and can identify the beta-emitting radioisotopes by means of their half-life and their beta energy spectrum. The detector is a plastic scintillator BC408 (BICRON, τ_{decay} = 2.1 ns, size 6 x 6 x 5 cm^3), optically coupled to a short photomultiplier tube (PMT, Hamamatsu R1924A), that is placed inside the vacuum chamber and is powered by an active voltage divider (Electron Tubes – PS 1807/5, Vpower = 6V) installed outside.

The CsI(Tl) and the plastic scintillator are mounted on the same holder, mechanically fixed to a steel rod that can slide vertically by means of a pneumatic actuator. Depending on the application (stable beam imaging, radioactive beam imaging, beam identification/counting), the device can be inserted in beam in three different operating positions or removed.

Figure 7.25: *Sketch and picture of the LEBI device*

When operating with radioactive beams, and in particular if the beam or some contaminant has a long decay time (several seconds or more), one would like to prevent its implantation onto the screen that would result in a long and impractical afterglow. For this reason an additional position of the screen was foreseen, allowing the beam to be implanted on a thin (6 μm) aluminized mylar tape that covers the lower half of the CsI(Tl) screen surface. Whenever needed, the tape can be rolled horizontally by means of a stepper motor, thus providing the screen with a fresh radiation-free portion of tape. The radiation emitted by the decay of the implanted beam particles (mainly β and γ rays), crosses the scintillating screen thus showing the beam profile. For beam species involving gamma decay channels, LEBI can be supplemented with one or two high purity coaxial germanium detectors (HPGe). Indeed, two hollow cups with thin windows, made from Ergal, allow to insert the HPGe heads down to 7 cm from the tape region where the beam is implanted, yet staying in air outside the beam pipe. This allows to perform gamma-ray spectroscopy in order to fingerprint the nuclear species present in the beam, thus providing a better characterization of the beam itself. Moreover, by knowing the branching ratios related to the involved gamma levels and the relative detector efficiency (70% for our detectors), the beam intensity can be inferred. Two germanium detectors are quite useful for radionuclides emitting gamma cascades, as the background can be strongly suppressed by imposing a coincidence: by means of such a procedure selected gamma levels can be enhanced in the resulting spectrum. The management of all the LEBIs installed along the beam line and their associate equipment is performed by means of rack computers, that are installed along the beam line. They drive the mechanical actuators, the motors for winding the mylar tape, the power supplies, the PMT data acquisition, the video signals from CCD cameras. All of this equipment is controlled by software code developed in LabView environment, which implements a friendly Graphical User Interface (GUI) currently operated by the accelerator crew without any special training.

The imaging sensitivity for stable beams was measured by decreasing the beam energy at the lowest allowed value, i.e. 5 keV, and then decreasing the intensity until the beam spot was barely detectable. The measured sensitivity limit at 5 keV of the pilot ^{7}Li beam, roughly corresponds to a flux of 10^{4} pps/mm^{2}, that is a power released in the screen of about 10 pW/mm^{2}.

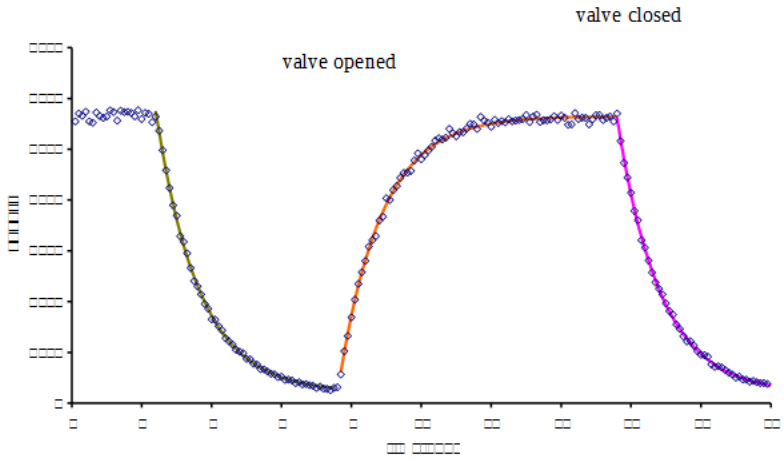

Figure 7.26. *Beam profiles and decay curve as measured in real time with the LEBI*

Switching on and off the beam impinging onto the plastic scintillator, it is possible to reconstruct the profile of the beta decay curve, such in the case of the ^{8}Li beam. After opening the valve it is possible to observe the exponential increase of the counting rate, whose value becomes stable after roughly 5 times the mean lifetime for particle decay **τ**, Fig. 7.26. By integrating the counts for a time interval of 1 second and correcting for the efficiency of 48 $\pm$ 1 %, as calculated with the PENELOPE MonteCarlo code, the value of the beam rate could be measured on each device in real time.

By taking into account the peculiarities of the ^{132}Sn (Fig. 7.27), kept as reference of a SPES beam, we have outlined a design based in a first approach on some of the following detectors to be assembled into a multisensor device:

- CsI(Tl) screen for beam imaging
- Plastics scintillator for beta counting
- CdTe solid state detector for low energy gamma counting
- LaBr3(Ce) scintillator coupled to a PMT for accurate gamma spectroscopy
- Germanium detectors
- Detectors for coincidence/anticoincidence triggers.

The price of each device, including mechanics, detectors and electronics, should be about 30 keuro, excluding the germanium detectors.

The aim is the measurements of all the beam parameters needed for an efficient beam transport, with the same approach of the LEBI's.

Figs.7.28) and 7.29) shown the position where we expect to install the diagnostic box. According with the EXCYT experience it is convenient to have some extra devices to simplify the difficult job of low intensity beam transport.

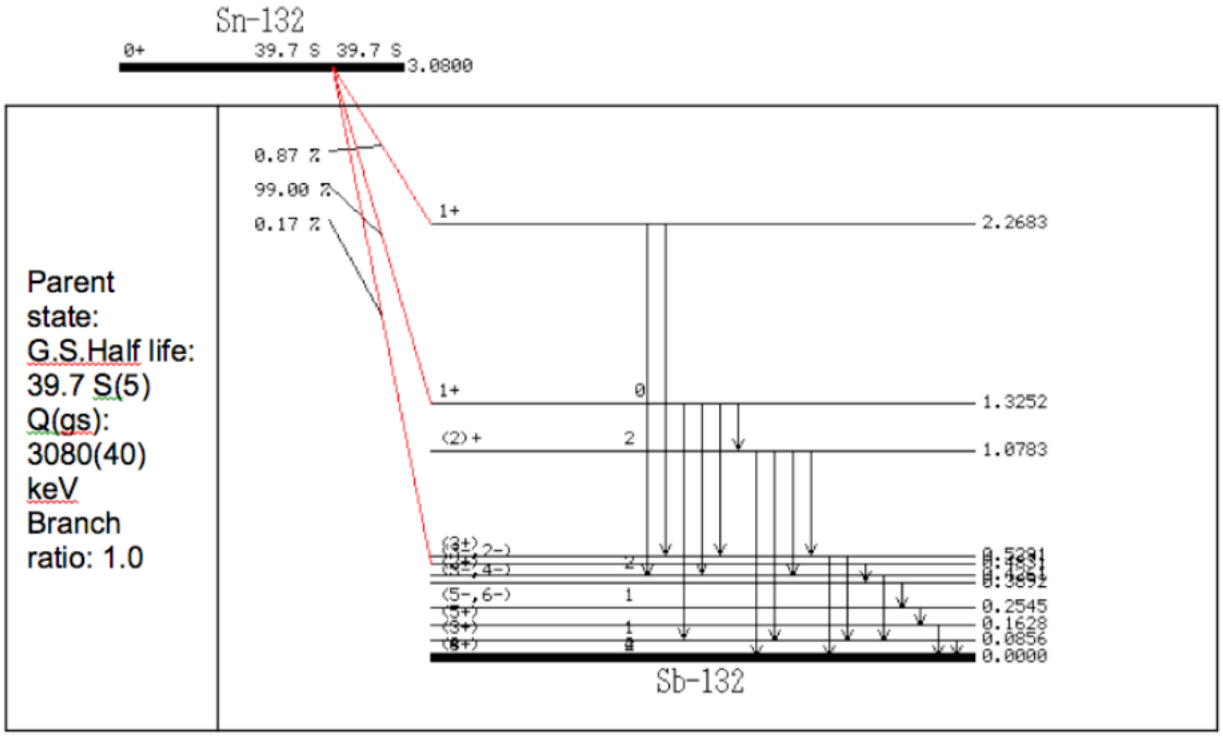

Figure 7.27: *Decay scheme of the ^{132}Sn beam.*

7.7 Vacuum Pumps

According to the fig. 7.28 and 7.29) we have to transport the beam through a long beam transfer line, about 80 m excluded HRMS. Moreover the beam energy is quite low 40 keV, so it is mandatory to achieve a good vacuum along the whole beam line to minimize the beam losses of our precious particles. Our vacuum goal is $<1\times10^{-7}$ Torr. The vacuum system choosen to perform this goal consists of a turbo pump (turbo MAG W600P – DN 160 CF, of Oerlikon Leybold), of a dry rough pump Alcatel Adixen ACP 28 and by vacuum gauge IKR 060 and TPR 018. Each pumping system will be connected to the beam line through a vacuum gate valve DN-160. The pumping system will be located generally at the same position where will be installed the main diagnostic boxes and are indicated by the red circles in fig. 7.28 and 7.29.

On the next weeks a pumping system module will be connected to a module of beam line transport made by a quadrupole electrostatic triplet and two beam line tubes with length of 3 m each to measure the level of vacuum achievable. Additional test will be done including the diagnostic box.

According to the fig. 7.28) and fig. 7.29) we need at least 17 vacuum pumping modules. HRMS and RFQ beam cooler excluded.

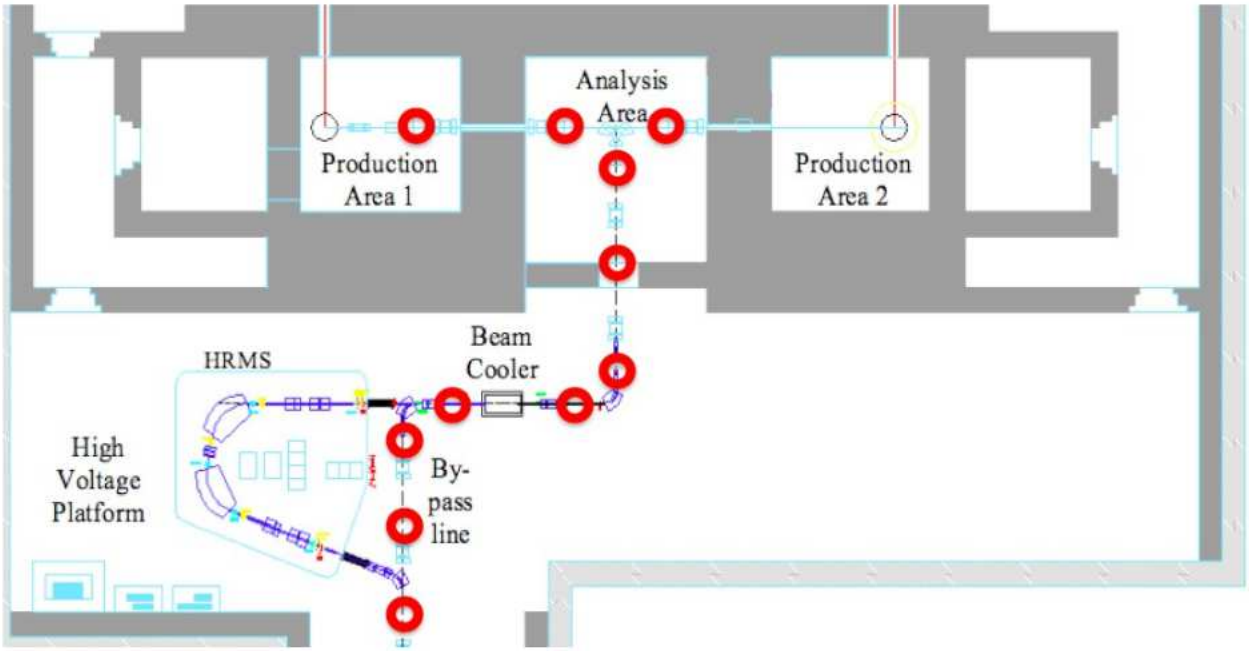

Figure 7.28: *Positions of the diagnostic box and of the main vacuum pumps along the beam transfer line from the ion source to the By-pass line. The red circles indicated the positions.*

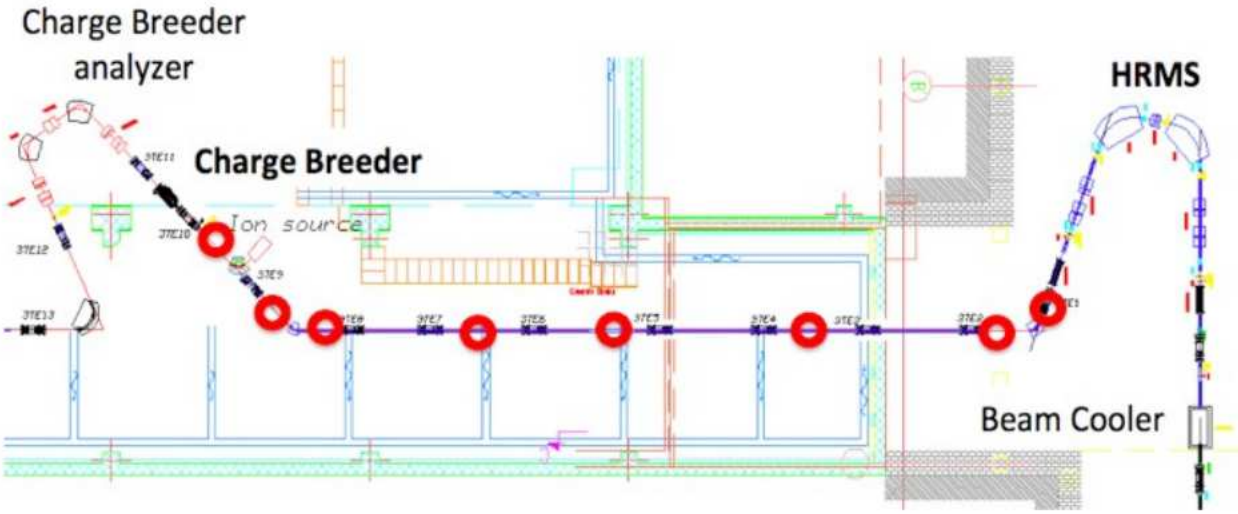

Figure 7.29: *Positions of the diagnostic box and of the main vacuum pumps along the beam transport line. The red circles indicated the positions.*

References

[1] GIOS code, H. Wollink
[2]R.B. Mooore et al., Nucl. Instr. and Meth. B 204 (2003) 557
[3] R.B. Mooore et al. Int. J. Mass Spectrometry 251 (2006) 190.
[4] O. Gianfrancesco, et al., Nucl. Instr. and Meth. B 266 (2008) 4483
[5] F.G. Major and H.G. Dehmelt, Phys. Rev. 170, 91 (1968)
[6] A. Andrighetto et al. "The SPES project at LNL" AIP Conf. Proc. 1099 pp. 728-732.
[7] A. Andrighetto et al., Eur.Phys. J. A 42, 517-521 (2009)
[8] A. Galatà INFN-LNL Annual Report 2011, 249
[9] M. Comunian et al., Proceeding of this Conference (HIAT2012), Chicago, USA.
[10] G. Bisoffi et al. Proceedings of this Conference, (HIAT2012), Chicago, USA.
[11] P. Hartmann et al., Plasma Source Sci. Technol. 9 (2000) 183.
[12] G.Audi et Al. Nuclear Physics A 729 (2003) 337–676.
[13] Cary N. Davis, Don Peterson, NIM B 266 (2008) 4449-4453.
[14] Cosentino L. et Al. , NIMA, Volume 622, Issue 3,Pages 512–517